THE QUASI-BIENNIAL OSCILLATION'S INFLUENCE ON LIGHTNING PRODUCTION AND DEEP CONVECTION IN THE TROPICS

A Thesis

by

CELINA ANNE HERNANDEZ

Submitted to the Office of Graduate Studies of
Texas A&M University
in partial fulfillment of the requirements for the degree of

MASTER OF SCIENCE

December 2008

Major Subject: Atmospheric Sciences

THE QUASI-BIENNIAL OSCILLATION'S INFLUENCE ON LIGHTNING PRODUCTION AND DEEP CONVECTION IN THE TROPICS

A Thesis

by

CELINA ANNE HERNANDEZ

Submitted to the Office of Graduate Studies of
Texas A&M University
in partial fulfillment of the requirements for the degree of

MASTER OF SCIENCE

Approved by:

Chair of Committee,	Courtney Schumacher
Committee Members,	Kenneth P. Bowman
	Jennifer Irish
Head of Department,	Kenneth P. Bowman

December 2008

Major Subject: Atmospheric Sciences

ABSTRACT

The Quasi-Biennial Oscillation's Influence on Lightning Production and Deep Convection in the Tropics.

(December 2008)

Celina Anne Hernandez, B.S, Texas A&M University

Chair of Advisory Committee: Dr. Courtney Schumacher

Variations in characteristics of tropical deep convection are examined for an association with the stratospheric quasi-biennial oscillation (QBO). Eight years (1998-2005) of Tropical Rainfall Measuring Mission (TRMM) Lightning Imaging Sensor (LIS) flash densities and ten years (1998-2007) of TRMM Precipitation Radar (PR) deep convective and stratiform rainfall and convective echo top heights are analyzed. The QBO can be linked to deep convection through two hypothesized mechanisms: 1) modulation of tropopause height, which may affect the altitude that convection can penetrate; and 2) modulation of cross-tropopause shear, which may affect the vertical development of convection via shearing of cloud tops. Tropopause height and cross-tropopause shear is measured by National Centers for Environmental Prediction (NCEP) reanalysis 100 hPa temperatures and 50-200 hPa zonal wind shear, respectively.

When partitioned by QBO east and west phases, zonal monthly mean anomalies and anomalous monthly mean difference maps illustrate a QBO signal in lightning flash rates, convective and stratiform rain amounts, and the number of convective echo tops >

12 km. QBO modulation of cross-tropopause shear causes 50-200 hPa shear east (west) phase anomalies to decrease (increase) about the equator and increase (decrease) in off-equator regions. QBO modulation of tropopause height induces a higher/colder (lower/warmer) tropopause near the equator during the east (west) phase. While the expectation was that decreases in cross-tropopause shear and tropopause temperatures at monthly time scales during the QBO would result in an increase of deep convective properties near the equator, observations suggest that deep convective properties may increase *or* decrease depending on the location and season. Similar to the QBO results, the increase or decrease of deep convective properties with general variations in cross-tropopause shear and tropopause temperatures depends on the location and season.

TABLE OF CONTENTS

1. INTRODUCTION

The Quasi-Biennial Oscillation (QBO) is a 24-30 month oscillation of the equatorial zonal winds in the lower stratosphere. During this period, zonally symmetric easterly (east phase) and westerly (west phase) wind regimes regularly alternate (Reed et al., 1961; Lindzen and Holton, 1968; Holton and Lindzen, 1972). The succession of the easterly and westerly regimes begins above 30km. Each regime propagates downward at an average rate of 1 km month^{-1}, with the westerly regime descending more regularly and rapidly than the easterly regime (Fig. 1; Baldwin et al., 2001). However, the easterly regime is stronger in intensity and has a longer duration. Observations show that the QBO's amplitude remains the same between 30 and 23 km with rapid attenuation beginning below 23 km. The QBO's amplitude has a maximum centered over the equator and is approximately Gaussian about the equator with a 12° half width (Wallace, 1973).

A QBO signal in temperature is evident in the tropics and extratropics (Baldwin et al., 2001). Closely associated warm and cold stratospheric temperature anomalies accompany the different wind regimes as they propagate lower into the atmosphere (Fig. 2; Gray et al., 1992). As Andrews et al. (1987) notes, the temperature QBO in the tropics is in thermal wind balance with the vertical shear of the zonal winds. The equation expressed for the equatorial β-plane is

---

This thesis follows the style of *Journal of Climate.*

$$\frac{\partial u}{\partial z} = \frac{-R}{H\beta}\frac{\partial^2 T}{\partial y^2}$$

where u is the zonal wind, T is temperature, z is log-pressure height, y is latitude, R is the dry air gas constant, $H \approx 7$ km is the nominal scale height used in the log-pressure coordinates, and β is the latitudinal derivative of the Coriolis parameter. The thermal wind balance for QBO variations on the equator is approximated by

$$\frac{\partial u}{\partial z} \sim \frac{R}{H\beta}\frac{T}{L^2}$$

where L is the meridional scale. Equatorial QBO temperature anomalies reach a maximum near 30-50 hPa and are on the order of ±4 K. Temperature anomalies associated with the QBO extend down to the tropopause and are of the order $\pm$0.5 K.

Lindzen and Holton (1968) showed that a broad spectrum of vertically propagating waves with eastward and westward phase speeds could drive the QBO. When forced by vertically propagating waves, their 2-D model produced an oscillation in the lower stratosphere through an internal mechanism involving a two-way feedback between the waves and the background flow. Rossby, mixed Rossby-gravity, and equatorial Kelvin waves were the first 2-D model run solutions to provide an explanation for the QBO (Baldwin et al., 2001). The first observations of equatorial Kelvin waves in the lower stratosphere were examined by Wallace and Kousky (1968). It was determined that the equatorial Kelvin wave produced an upward flux of westerly momentum, which could account for the west phase. Bretherton (1969) hypothesized that the east phase of the QBO could be attributed to the mixed Rossby-gravity wave. However, observations showed that the QBO could not attain a 24-30 month period with the forcing provided by

mixed Rossby-gravity and Kelvin waves alone. The additional momentum flux needed to correctly force the QBO required a broader spectrum of gravity waves (Dunkerton, 1997).

Quasi-biennial variability has been found in various tropical fields, i.e., rainfall, outgoing longwave radiation (OLR), and 200hPa zonal winds (Collimore et al, 1998). Further, the QBO has been postulated to influence deep tropical convection via changes in tropopause height (Collimore et al., 2003). As the easterly and westerly wind shear regimes propagate downward into the atmosphere, an anomalous meridional circulation is induced. Due to contrasting thermal regimes, hydrostatic effects in the lower and upper stratosphere may favor equatorial convection during the east phase (Gray et al., 1992). More specifically, the QBO's east (west) phase induces anomalous motion that leads to a cooler, higher (warmer, lower) tropopause near the equator (Fig. 3). Gray et al. noted that temperature anomalies in areas 10-20° off the equator are 180° out of phase with those near the equator. Therefore, strong east phase cooling near the equator is accompanied by a weak warming in off-equator regions. By this notion, it is anticipated that deep convection will increase (decrease) during the east (west) phase near the equator and decrease (increase) during the east (west) phase away from the equator.

Collimore et al. (2003) also argued that deep convection may be affected by the QBO's modulation of upper-tropospheric to lower-stratospheric wind shear (i.e., between 50 and 200 hPa). The east (west) phase of the QBO induces weak (strong) vertical shear in and near equatorial regions (Fig. 4). The reverse scenario is expected in off-equator regions. Upper-tropospheric zonal winds associated with the QBO show

some geographical variation near the equator (Collimore et al., 2003; Hamilton et al., 2004). Therefore, the increase/decrease of deep convection not only depends on the phase of the QBO but also on the location of convection. Weak shear will allow convection to extend further into the atmosphere while strong wind shear will shear cloud tops off (Fig. 5). Thus, the QBO's modulation of cross-tropopause shear is expected to allow deep convection to increase (decrease) during the east (west) phase in near equatorial regions and decrease (increase) during the east (west) phase in off-equator regions.

Because lightning is a response to thermodynamic and dynamic forcing, lightning observations can be used as a proxy for deep convection (Christian et al., 1999). For lightning to occur, a well-developed mixed-phase region is required. Deep, vigorous convection allows the zones of mixed-phase microphysics to be deeper and more developed, especially in the tropics (Mushtak et al., 2005). Therefore, lightning production is enhanced in deep convection. The depth of convective clouds is also an important factor in determining convective precipitation properties (Gagin et al., 1985; Rosenfeld and Gagin, 1989). In general, greater rainfall amounts are associated with deeper convection because of the increase of diameter of the convective cell and longer convective lifetimes. One might expect that an increase in the depth of convection by the QBO should be evident in lightning flash rates and convective echo tops and rainfall amounts.

This study focuses on examining the relationship between the QBO and tropical deep convection using observations from the Tropical Rainfall Measuring Mission

(TRMM) satellite. Flash densities, convective and stratiform rainfall, and convective echo top counts are composited into west minus east anomalous monthly mean difference maps for each season. It is hypothesized that lightning flash densities, deep convective rainfall amounts, and echo top heights will increase (decrease) during the east (west) phase near the equator and decrease (increase) during the east (west) phase in off-equator regions with different contributions from tropopause height and wind shear variations.

Section 2 will provide information on the data used and describe the methodology for the present study. An investigation of the relationship between the QBO and lightning will be presented in Section 3. Section 4 will present an analysis of the relationship between the QBO and deep convection through radar-derived echo top heights and rainfall amounts. Finally, the conclusions will be discussed in Section 5.

2. METHODS

2.1 Instruments

This study uses observations from the TRMM satellite to examine the relationship between the QBO and flash densities for eight years (1998-2005) and deep convective rainfall and echo top counts for ten years (1998-2007) between 20°N and 20°S. The area between 10°N and 10°S is labeled the near-equatorial region, while the areas between 20°N and 10°N and 10°S and 20°S are labeled as off-equator regions. Flash densities are retrieved by the Lightning Imaging Sensor (LIS) onboard the TRMM satellite. Rainfall amounts and echo top heights are retrieved by the TRMM Precipitation Radar (PR).

LIS contains a staring imager that is able to detect lightning with storm-scale resolution of 3 km at nadir and 6-km at limb (Christian et al., 2000). The field-of-view can observe a point on the Earth or a cloud for 80 seconds, which provides enough time to estimate the flashing rate of storms. For each lightning event, LIS will record the time of occurrence, measure the radiant energy, and estimate the location. A real-time event processor removes the background signal and thus enables the system to detect weak lightning. The real-time event processor allows the LIS instrument to achieve 90% detection efficiency.

The PR operates at 13.8 GHz and is the first quantitative precipitation radar to be placed in space. The PR's orbit was boost from an altitude of 350 km to 400 km in August 2001 and has a 4.3 km pre-boost/5 km post-boost nadir field-of-view and a 220

km pre-boost/245 km post-boost swath width (Okamoto et al., 2004). The PR makes 16 orbits per day and covers a 38°N to 38°S latitudinal band from 180°W to 180°E. The PR has a precessing orbit so that it can capture the full diurnal cycle. It is the only instrument on the TRMM satellite that can directly observe vertical distributions of rain. The PR is also able to retrieve quantitative rainfall estimation over land and ocean.

2.2 Data

TRMM LIS flash densities are obtained from the Global Hydrology Resource Center (http://thunder.msfc.nasa.gov/data). The Low Resolution Monthly Time Series (LRMTS) comes binned in a 2.5° x 2.5° grid. As of present, LIS LRMTS data is only available from 1998-2005.

The 2A23 and 2A25 V6 PR orbital data are taken from NASA's TRMM Data Access site (http://daac.gsfc.nasa.gov/data/datapool/TRMM_DP). The 2A23 V6 PR product provides the echo-top height of convection as well as the rain-type classification for each precipitation event. The algorithm for the rain-type classification compares the vertical and horizontal distribution of radar reflectivity (Steiner et al., 1995; Awaka et al., 1997). Houze (1981) showed that large vertical and small horizontal structures of high reflectivity are associated with convective rain. However, the reflectivity structure associated with stratiform rain is a horizontally homogeneous region of weak to moderate reflectivity and often contains a brightband around the melting level. Due to a minimum sensitivity of ~17 dBZ, the PR does not see true cloud top, which should be taken into consideration when viewing the echo-top statistics in Section 4.

The 2A25 V6 PR product provides the attenuation-corrected reflectivity from 0-20 km in altitude with 250 m vertical resolution (Iguchi et al., 2000). For each orbit, the latitude, longitude, height, reflectivity, and echo top height for each rain type are composited into daily and monthly 5-D histograms. In order to avoid the effects of surface return and attenuation, this study only considers rainfall retrievals at 2 km. Tropical convective and stratiform rain rates are calculated from the attenuation-corrected reflectivity using $Z=148R^{1.55}$ and $Z=276R^{1.49}$, respectively where Z is the reflectivity factor and R is the rainrate. In addition, Shimizu et al. (2003) showed differences between pre-boost and post-boost TRMM PR rainfall trends to be negligible.

Monthly mean temperature and zonal wind data are taken from the National Centers for Environmental Prediction-National Center for Atmospheric Research (NCEP-NCAR) reanalysis (Kalnay et al., 1996). NCEP data is interpolated and remapped into 2.5° x 2.5° grids to match the TRMM LIS and PR data binning. The phases of the QBO are defined by a zonal mean equatorial zonal wind 50-70 hPa shear index (Fig. 6). This index is used because the mechanisms linking the QBO to deep convection occur in and near the tropopause (Huessmann and Hitchman, 2001; Collimore et al., 2003). Approximately two-thirds of the asymmetry in the wind shear zone descent rate is eliminated when removing the time mean and annual cycle. West phase months are defined as months with 50-70 hPa shear values ≥ 1.5 m s^{-1}. Months in the east phase have 50-70 hPa shear values ≤ -1.5 m s^{-1}. The LIS (PR) eight (ten) year period contains three (four) full QBO cycles. Although the results may be sensitive to the number of QBO cycles, this analysis is restricted to using an eight and ten year study

period due to the length of the TRMM datasets. Using a 23-year OLR dataset, Collimore et al. (2003) found that ENSO biasing of west minus east QBO convective patterns was weak. However, it was noted that a longer dataset was required to truly determine the effect of ENSO on QBO west minus east convective patterns. Due to the length of the datasets used in this study, the relationship between ENSO and the QBO will not be examined.

In order to measure the QBO's modulation of cross-tropopause shear, an absolute 50-200 hPa shear is calculated. The absolute values of the 50-200 hPa shear are taken due to the geographical variation of the zonal winds. Tropopause temperatures are defined as temperatures at the 100 hPa level. Absolute 50-200 hPa shear values and tropopause temperatures are then composited into west minus east anomalous monthly mean difference maps for each season.

The QBO's influence on convective characteristics is tested by correlations for each geographical region and season. Maps of correlation coefficients between lightning, convective rainfall, stratiform rainfall, and convective echo tops and cross-tropopause shear and tropopause height were also created to further investigate the relationship between convective responses and the basic mechanisms that influence deep convection.

3. THE QBO'S INFLUENCE ON LIGHTNING PRODUCTION IN THE TROPICS

In order to determine if a QBO signal is present in lightning, zonal monthly mean anomalies averaged for the QBO's east (dashed) and west (solid) phase were calculated for LIS flash densities (Fig. 7a). Each zonal mean anomaly is calculated with a 2.5° latitudinal resolution. East (west) phase flash density anomalies are negative (positive) in the near-equatorial region, implying that lighting production decreases (increases) during the east (west) phase. Near-equatorial east and west phase magnitudes are largest between the equator and 6°S. Flash density anomalies are weaker away from the equator in both the Northern and Southern Hemisphere and switch signs in the Southern Hemisphere at 14°S. Comparison of mean monthly flash densities (Fig. 8) and zonal monthly mean anomalies indicates that the variations of lightning during the QBO range from 0.5%-2.5%.

As previously discussed, QBO modulation of cross-tropopause shear and tropopause height may influence the height of deep convection (and thus lighting production). Figure 7b shows that zonal mean 50-200 hPa shear anomalies decrease (increase) during the east (west) phase between 6°N and 8°S with opposite relationships poleward of these latitudes. Figure 7c shows that the zonal mean tropopause is higher/colder (lower/warmer) than normal between 14°N and 20°S. Comparison of flash density, cross-tropopause shear, and tropopause height zonal mean anomalies are *inconsistent* with the hypothesized relationship between the QBO and lightning. For

example, near the equator lightning production decreases during the east phase when shear is weaker and heights are higher.

While zonal mean values of lightning production and the QBO modulation of cross-tropopause shear and tropopause height did not have the expected relationship, the zonal mean anomalies still show a QBO signal in lightning. Further, zonal mean anomalies do not illustrate the longitudinal or seasonal variations of flash density magnitudes or patterns. Maps of west minus east flash densities, absolute 50-200 hPa shear, and tropopause temperatures for each season are given in Figs. 9-11. In general, the seasonal difference maps show the largest signals over land because of the much higher lightning flash densities observed over land (Fig.8). Therefore, this analysis focuses on four land regions: Africa, India, Maritime continent/Australia, and South America.

3.1 Africa

West minus east flash density anomalies for DJF (Fig. 9a) show a large increase in lightning in the Congo and a moderate increase in southern Africa and Madagascar during the east phase. Flash densities moderately increase during the west phase along the west coast of Africa. Comparison of Figs. 9a, 10a, and 11a indicate that the east phase signal over the Congo basin and west phase signals in the southern off-equator region are physically consistent with the QBO's modulation of DJF cross-tropopause shear and tropopause height in at least some parts of Africa. That is, flash densities are increasing when cross-tropopause shear is decreasing and the tropopause height is

reaching higher altitudes. For example, the decrease in shear and temperatures during the east phase near the equator corresponds with the east phase signal in lightning.

In contrast to DJF, MAM flash densities over the Congo basin increase during the west phase (Fig. 9b). In addition, much of west and east Africa shows an east phase signal in flash densities. However, both the near-equatorial west phase signal and east phase signal above 10°N cannot be attributed to either hypothesized QBO mechanism. Similar to DJF, MAM cross-tropopause shear and temperature difference maps indicate stronger shear and a lower/warmer tropopause in the near-equatorial region during the west phase (Figs. 10b and 11b).

Unlike DJF and MAM, JJA shows a pronounced increase in flash densities during the west phase over much of Africa (Fig. 9c). Strong west phase shear is present over the near-equatorial region, while the northern and southern off-equator regions experience stronger shear during the east phase (Fig. 10c). The QBO temperature difference map indicates a warmer/lower tropopause during the west phase throughout the entire region (Fig. 11c). Since JJA is the active monsoon season, it is possible that monsoon dynamics overwhelm shear and tropopause height variations in lightning production.

In general, SON flash densities north of the equator in Africa increase during the west phase, while flash densities south of the equator increase during the east phase (Fig. 9d). The SON shear and temperature west minus east patterns are similar to other seasons, with the exception of a narrow west phase shear band along eastern Africa (Figs. 10d and 11d). The increase of flash densities when strong shear is mostly present

suggests that QBO modulation through shear has a reversed influence on lighting production in Africa during SON. Comparison of QBO flash density and tropopause temperature observations indicates that lightning in the near equatorial region weakly increases when the tropopause is higher/colder during the east phase.

Tables 1 and 2 give the seasonal correlations between lightning flash density and 50-200 hPa shear and tropopause temperature for Africa. With the exception of DJF, correlation coefficients in Africa range from weak-to-moderate positive values suggesting that other factors such as the monsoon are overwhelming the influence of cross-tropopause shear and tropopause height variations on deep convection during the QBO. Although not statistically significant, the DJF cross-tropopause shear correlation of -0.11 suggests that the strongest relationship between QBO modulation through shear is seen over Congo.

3.2 India

Flash densities generally increase over the Indian subcontinent during the west phase year round (Fig. 9). However, there is a lack of a QBO signal during DJF, likely due to the absence of deep convection during that season, and southern India experiences lightning increases during the east phase in MAM. The increase in flash densities during the east (west) phase in MAM may be attributed to the weak east (west) phase shear present over the subcontinent (Fig. 10b). Comparison of QBO temperature and flash densities in MAM indicate that QBO modulation through height only influences lightning during the east phase in the southern portion of the subcontinent (Fig. 11b).

While west minus east JJA and SON difference maps illustrate a weak QBO west phase signal over the Indian subcontinent (Figs. 9c and d), cross-tropopause shear patterns show stronger shear during the west (east) phase over the southern (northern) subcontinent (Figs. 10c and d). QBO temperature anomaly difference maps show a warmer/lower tropopause throughout the subcontinent during the west phase (Figs. 11c and d). Observations of shear decreasing and flash densities increasing during the west phase in the northern subcontinent indicate QBO modulation through shear influences flash density patterns in this region. The JJA and SON west phase increase of flash densities with a west phase lower tropopause suggests QBO modulation through height does not play a role in altering Indian lightning patterns.

Compared to Africa, Indian seasonal correlation coefficients are predominantly negative (Tables 1 and 2). The MAM correlation suggests that QBO modulation through shear may have a weak-to-moderate influence on lightning production (although the tropopause temperature correlation during MAM has an opposite sign). The strongest relationship between the QBO and Indian flash densities occurs during JJA as indicated by the high negative values of both QBO mechanism correlations. It is noted that JJA is India's active monsoon season, but that correlations during the Indian monsoon season are opposite of W. Africa's monsoon season.

3.3 Maritime Continent/Australia

A DJF flash density QBO west phase signal occurs over the Maritime continent, and the west coast of Australia (Fig. 9a). Central and East Australia show an intense

increase in flash densities during the east phase. Absolute 50-200 hPa shear anomalies (Fig. 10a) indicate strong west phase shear over the Maritime continent, while temperature anomalies (Fig. 11a) exhibit a lower west phase tropopause over the entire region. Contrary to expectations, flash densities over the Maritime continent increase during the west phase when shear is strong and the tropopause is low. However, the west phase lightning signal in the southern off-equator region, i.e., below 10°S, is associated with weak west phase shear. A higher/colder tropopause during the east phase is associated with an increase in flash densities over central and east Australia.

Flash densities in MAM moderately increase during the east phase over Indonesia and weakly increase during the west and east phase in western and eastern Australia, respectively (Fig. 9b). The east phase increase in flash densities over Indonesia occurs when cross-tropopause shear is weaker (Fig. 10b). Further comparison of flash density and cross-tropopause shear monthly mean anomalies indicate that the increase in west and east phase signals over Australia occurs when shear is stronger during the east phase. Therefore, with the exception of the Australian east phase signal, flash density patterns are associated with QBO modulation through shear. Similar to DJF, the tropopause is lower/warmer during the west phase over the entire region. Therefore, QBO modulation through height is associated with the east phase increase in flash densities in the region.

Figure 9c shows a small area of weak west phase flash densities over Indonesia and some of the larger islands in the Maritime continent during JJA. A west phase signal is present in both shear and temperature anomaly plots, i.e., cross-tropopause shear is

stronger and the tropopause is lower during the west phase (Figs. 10c and 11c). Thus, the QBO mechanisms hypothesized to modulate lightning seem to produce the reverse flash density patterns.

The larger islands in the Maritime Continent and the west coast of Australia have a west phase increase in flash densities in SON (Fig. 9d). Flash density anomalies over the smaller islands in Indonesia and the majority of Australia moderately increase during the east phase. As with previous seasons, the weak east phase signal in Indonesia and west phase signal in Australia occurs when shear is weak during their respective phase (Fig. 10d). Temperature and flash density anomaly maps indicate that the large east phase signal in Australia is potentially influenced by QBO modulation through height (Fig 11d). However, neither mechanism is able to account for the strong west phase signal over the larger islands of the Maritime continent.

With the exception of MAM shear, Maritime Continent/Australia correlations are positive (Tables 1 and2), especially during JJA and SON when west phase flash density patterns are seen throughout the region. The MAM shear correlation supports the weak east phase enhancement of flash densities over Sumatra when cross-tropopause shear is weak. It is therefore suggested that factors other than the hypothesized role of cross-tropopause shear and tropopause height variations during the QBO play a larger role in altering lightning production over the Maritime Continent/Australia.

3.4 South America

The DJF QBO signal alternates between the east and west phase throughout S. America (Fig. 9a). Northern S. America and the Amazon experience weak east and west phase enhancement of flash densities, respectively. However, flash densities in Brazil are strongly enhanced by the east phase and west phase. QBO cross-tropopause shear patterns reveal a "bulls-eye" of strong west phase shear over the Amazon (Fig. 10a). The remainder of S. America experiences stronger shear during the east phase, with an east phase maximum occurring along the east coast of Brazil. Tropopause temperatures are predominantly warmer during the east phase throughout the region (Fig. 11a). Since shear and temperatures increase during the east phase, neither QBO mechanism accounts for the weak and strong east phase enhancements seen in Fig. 9a. The weak west phase enhancement of lightning in the Amazon may be linked to the raising of the tropopause during the west phase. The intense west phase signal in eastern Brazil occurs in an area where west phase shear intensity is at a minimum and tropopause temperatures are colder. While the minimum in cross-tropopause shear leads to an intense west phase enhancement, QBO modulation through height can be associated with both the weak and strong west phase enhancement seen in the Amazon and eastern Brazil.

In MAM, flash densities tend to increase during the east phase with the exception of the west phase signal in northeastern Brazil (Fig. 9b). Absolute 50-200 hPa shear anomalies are positive over the Amazon basin, i.e., shear is stronger during the west phase (Fig. 10b). The east phase lightning signal in the western Amazon basin and west phase lightning signal in Brazil take place when shear is weaker during their respective

QBO phase. West minus east temperature anomalies are warmer during the west phase over most of the continent, with the exception of warmer east phase temperatures from 10°S to 20°S (Fig. 11b). East phase flash densities in the western Amazon are associated with a higher tropopause. Contrary to expectations, the southern east phase flash density enhancement occurs when shear is stronger and the tropopause is lower during the east phase.

As with previous seasons, the JJA west minus east flash density map exhibits a combination of west and east phase signals throughout the continent (Fig. 9c). The cross-tropopause shear difference anomaly difference map (Fig. 10c) reveals a narrow band of west phase shear that extends through the center of the Amazon basin. Cross-tropopause shear anomalies are negative everywhere outside of this narrow band. The tropopause is higher during the east phase throughout the entire region (Fig. 11c). Comparison of absolute 50-200 hPa shear and flash density anomalies reveals that modulation through cross-tropopause shear may influence a portion of the east and west phase lightning signal near the Amazon basin. The evaluation of the temperature and lightning difference maps indicates that the relationship between lightning and temperature is weaker than that with cross-tropopause shear.

Similar to DJF and JJA, SON flash density QBO signals alternate from east and west phase enhancements throughout S. America (Fig. 9d). With the exception of MAM, it is noted that the Amazon consistently exhibits a west phase enhancement of flash densities. The consistent west phase signal in the Amazon may in part be due to the dynamics associated with the Amazon basin's marine-like environment (i.e., west phase

signals seem to predominate in coastal regions and inland during the active monsoon, situations when maritime conditions strongly influence the nature of convection). A portion of the northwest east phase signal can be linked to the small area of decreased east phase shear in northwest S. America (Figs. 10d). Because parts of the strong west phase enhancement over the Amazon occur in an area of weak west phase shear, QBO modulation through shear may influence flash densities in the western Amazon. Supporting the QBO hypothesis, the east phase signals above 10°S are linked to a higher/colder tropopause during the east phase (Figs. 11d). Neither mechanism is associated with the east phase enhancement of lightning in the southern off-equator region.

Table 1 shows that cross-tropopause shear versus flash density correlations are weak during each season. Further, tropopause temperatures versus flash density correlations are also fairly weak (Table 2), with the exception of SON. Fig. 9 illustrated a variable and local relationship between the QBO's mechanisms and flash densities. Therefore, correlations are expected to be low since a clear overall relationship between the QBO and flash densities cannot be found over the S. American region.

3.5 Flash Densities and Variations in Cross-tropopause Shear and Tropopause Height

The previous discussion examined the relationship between the QBO's hypothesized mechanisms and flash densities. But how much do the variations in absolute 50-200 hPa shear and tropopause temperatures alter flash density production in

a more general sense? To address this question, correlation coefficient maps of monthly lightning and cross-tropopause shear and tropopause temperatures were constructed (Figs. 12 and 13). Negative (positive) correlations indicate an increase in flash densities when cross-tropopause shear is decreasing (increasing) and the tropopause is higher/colder (lower/warmer).

Figure 12 shows that African cross-tropopause shear correlations are generally weak year round; thus, indicating a weak relationship to flash densities. However, moderate-to-strong negative correlations in MAM (Fig. 12b) imply that a decrease in cross-tropopause shear is associated with a large enhancement of flash densities. The opposite is true in JJA (Fig. 12c). Over India, weak correlations in MAM and SON along with near-zero correlations in DJF and JJA suggest that Indian flash densities are not strongly associated with 50-200 hPa shear variations, although the signal of positive values over northern India and negative values over southern India is consistent between MAM and SON. Figure 12 also shows the Maritime continent generally experiencing an increase in flash densities when cross-tropopause shear increases throughout the year. With the exception of DJF, near-zero coefficients in Australia indicates that shear variations do not have much of a relationship with Australian lightning. Only in DJF does the variation of cross-tropopause shear weakly correlate with lightning production in central and eastern Australia (Fig. 12a). MAM and JJA northwest S. American flash densities are strongly correlated to cross-tropopause shear (Figs. 12b and c). Correlations of -0.8 and -1.0 imply that cross-tropopause shear is in large part responsible for flash density variations in northwest S. America. As with the QBO discussion, it appears that

decreases in cross-tropopause shear at monthly time scales can be associated with increased or decreased lightning production depending on the location and season.

Figure 13 shows moderate negative correlations in DJF and MAM over Africa, which indicate that a decrease in temperatures is associated with a modest increase in lightning. As with cross-tropopause shear, JJA shows an opposite signal. The Indian subcontinent exhibits a modest increase of flash density production when tropopause temperatures are colder during MAM and SON (Fig. 13b and d). DJF and MAM moderate negative correlations suggest a modest enhancement of lightning in Indonesia when temperatures are decreasing (Figs. 13a and b). However, predominantly positive correlations in the Maritime continent during JJA and SON suggest a reversed influence between lightning and temperature variations (Figs. 13c and d). Australian correlations are somewhat opposite of the Maritime continent's during DJF and SON. S. America exhibits regions of moderate-to-strong negative correlations year round. DJF flash densities in eastern Brazil are strongly associated with the decrease in tropopause temperatures (Fig. 13a). Similar to cross-tropopause shear correlation patterns, MAM flash densities experience the strongest link to decreasing tropopause temperature variations in northwest S. America (Fig. 13b). Moderate negative correlations occur in central S. America during JJA and SON (Figs. 13c and d).

4. THE QBO'S INFLUENCE ON TROPICAL CONVECTIVE AND STRATIFORM RAIN AND CONVECTIVE ECHO TOP HEIGHTS

This section examines the QBO's relationship to convective and stratiform rain and convective echo top heights in the Tropics. As mentioned in Section 1, the depth of convective clouds is an important factor in determining other convective cloud properties, e.g., greater rainfall totals are associated with deeper convection (Gagin et al., 1985; Rosenfeld and Gagin, 1989). Therefore, PR convective rain, stratiform rain, and convective echo top monthly mean anomalies are examined in relation to the QBO and the QBO's hypothesized influences on deep convection. Figure 2 illustrates that the QBO can affect convective clouds that reach 200 hPa. It is therefore expected that the number of convective echo top heights above 12 km increases (decreases) during the east (west) phase, with concomitant increases (decreases) in convective and stratiform rainfall.

Figure 14 shows the zonal monthly mean anomalies averaged over the QBO east and west phases for convective and stratiform rain, convective echo top count, and the corresponding ten years (1998-2007) of absolute 50-200 hPa shear and tropopause temperatures. East phase zonal mean convective and stratiform rainfall anomalies (Figs. 14a and 14b) are positive near the equator (i.e., between 8°N and 5°S) with magnitudes of 1-2 mm. Convective and stratiform rainfall anomalies hover closer to zero in the off-equator regions. West phase anomalies are generally opposite of the east phase pattern, although there is less of a signal in the west phase north of the equator compared to the

east phase. Convective and stratiform rain monthly means are 50 mm and 35 mm, respectively. Therefore, variations during the QBO account for 4% of convective rainfall and 6% of stratiform rainfall. Unlike the convective and stratiform zonal monthly mean rainfall anomalies, the west and east phase zonal mean convective echo top counts are not symmetric about the equator (Fig. 14c). Rather, convective echo top zonal mean anomalies show the largest phase difference between 20°N and 10°N with magnitudes of 5-7 counts (compared to convective echo top monthly means of 20 counts). Convective echo top anomalies decrease toward the equator and show virtually no signal in the Southern Hemisphere.

Zonal monthly mean absolute 50-200 hPa shear and tropopause temperature anomalies during the PR observational period (1998-2007; Figs. 14d and 14e) are similar to the zonal mean anomalies during the LIS observational period (1998-2005; Figs. 7c and 7d). The east phase increase of convective and stratiform rainfall near the equator corresponds well with the east phase decrease in cross-tropopause shear and temperatures; however, the convective echo top zonal mean anomalies do not correspond as well.

Figure 14 gives evidence of a QBO signal in tropical stratiform and convective rain and convective echo tops. However, the zonal mean anomalies discussed above do not address the geographical or seasonal variations of deep tropical convective characteristics. Maps of west minus east convective rain, stratiform rain, convective echo top heights, absolute 50-200 hPa shear, and tropopause temperatures for each season are given in Figs. 15-19. Unlike the west minus east LIS anomalies, convective

and stratiform rain difference maps illustrate a robust QBO signal over the oceans. Therefore, the evaluation between the QBO and deep convective rain will primarily focus on the following regions: the Indian Ocean, Maritime continent, W. Pacific, South Pacific convergence zone (SPCZ), and Pacific and Atlantic intertropical convergence zones (ITCZs). However, the west minus east convective echo top height map exhibits a combination of land and ocean QBO signals. Thus, the evaluation of the QBO's influence on convective echo top heights focuses on interesting land and ocean features during each season.

4.1 The QBO's Influence on Convective Rainfall

The west minus east convective rainfall DJF anomaly map exhibits two large QBO signals (Fig. 15a). The first being the west phase enhancement of convective rainfall that begins in the western Indian Ocean and extends into the Maritime continent. The Indian Ocean west phase enhancement takes place within an area of stronger west phase shear (Fig. 18a). In addition, QBO temperature difference anomalies over the Indian Ocean and Indonesia indicate a lower/warmer tropopause during the west phase (Fig. 19a). Thus, the Indian Ocean signal does not correspond with the hypothesized QBO mechanisms. The second robust QBO signal begins in the eastern half of the Maritime continent and extends into the W. Pacific and SPCZ. Following with expectations, convective rainfall, absolute 50-200 hPa shear, and tropopause temperature anomaly maps indicate that the eastern Maritime continent and W. Pacific east phase enhancement may be linked to the decrease in shear and rise of the tropopause during the

east phase. However, a portion of the east phase increase in convective rainfall along the SPCZ materializes in an area of strong east phase shear and warmer east phase temperatures. A weak-to-moderate east phase signal is also seen extending from the Congo to southeast Africa and in the E. Pacific and Atlantic ITCZs.

The QBO signal that encompasses the Maritime continent, W. Pacific, and SPCZ transitions from a distinct east phase signal during DJF to a predominantly west phase signal in MAM (Fig. 15b). The opposite happens over the Indian Ocean. A switch from east phase to west phase enhancement also occurs in the E. Pacific, northern S. America, and Atlantic. Positive shear anomalies indicate that cross-tropopause shear strengthens during the west phase over the Indian Ocean, Maritime continent, W. and E. Pacific, northern S. America and the Atlantic during MAM (Fig. 18b). The west minus east MAM temperature map indicates warmer west phase temperatures throughout the near-equatorial region (Fig. 19b).

Compared to the previous seasons, JJA QBO convective anomalies are shifted towards the Northern Hemisphere (Fig. 15c). The JJA convective rain anomaly map reveals the following two robust QBO signals: 1) an east phase enhancement extending from the Indian Ocean to the Maritime continent and 2) a west phase signal north of the Maritime continent that continues across the Pacific basin. The east phase enhancement of convective rainfall over the Indian Ocean and Maritime continent corresponds with weaker east phase cross-tropopause shear and colder east phase tropopause temperatures (Figs. 18c and 19c). Because shear and temperatures in the W. Pacific increase during the west phase, the west phase signal seen in this region cannot be linked to the

hypothesized QBO mechanisms. The west phase increase along the ITCZ in the central Pacific corresponds with a decrease in west phase shear. However, the ITCZ QBO signal cannot be associated with QBO modulation through height, i.e., temperatures increase during the west phase throughout the Pacific.

The SON west minus east convective rain anomalies map exhibits a QBO west phase signal in the Indian Ocean, north SPCZ, and Pacific ITCZ and a QBO east phase signal in the Maritime continent and W. Pacific (Fig. 15d). A decrease of cross-tropopause shear during the QBO is associated with the large east phase signal that extends from Indonesia to the W. Pacific, the north SPCZ west phase signal, and the west phase signal in the central Pacific. However, the increase in cross-tropopause shear during the west phase over the Indian Ocean exhibits a reversed QBO relationship on convective rain in these regions. Tropopause temperatures are warmer during the west phase throughout the near-equatorial region and most of the off-equator regions. Therefore, the large east phase signal extending from Indonesia to the W. Pacific is the only QBO signal that may be linked to an increase in tropopause heights.

Tables 3 and 4 provide the correlations between convective rainfall and QBO modulation of cross-tropopause shear and tropopause temperature for each season and region. Weak correlations in Table 3 suggest a generally weak relationship between QBO modulation of 50-200 hPa shear and convective rainfall. However, negative correlations (i.e., values <~ -0.25) over Africa, the E. Pacific, and the Atlantic during DJF, the Maritime continent and E. Pacific during JJA, and the Atlantic during SON suggest that some regions experience increased convective rain during months of

decreased cross-tropopause shear associated with the QBO. Moderate positive correlations (i.e., values ~> 0.25) over the W. Pacific in DJF, Central and S. America and the Atlantic during MAM, and the Indian Ocean during SON imply a relationship reverse from expectations between convective rainfall and QBO modulation of shear. Correlations in Table 4 also suggest a generally weak relationship between QBO modulation of tropopause temperatures and convective rainfall. However, moderate negative correlations over the Maritime continent, W. Pacific, and SPCZ show an increase in convective rain when tropopause temperatures are colder in at least a few seasons. Moderate positive correlations occur over the E. Pacific in DJF and the Atlantic in MAM suggesting an increase in convective rain may be related to warmer QBO temperatures.

4.2 The QBO's Influence on Stratiform Rainfall

In general, QBO stratiform rainfall variations are similar to the variations seen in convective rainfall (Figs. 15 and 16). However, QBO stratiform variations in the Pacific ITCZ in DJF, the northwest Pacific in DJF and MAM, the Indian Ocean in MAM, and the southern SPCZ in JJA and SON exhibit different patterns than those seen in Fig. 15. Stratiform rainfall anomalies over the Pacific ITCZ illustrate a robust QBO west phase signal during DJF (Fig. 16a). DJF cross-tropopause shear anomalies are stronger during east phase (Fig. 18a) tropopause temperatures become warmer during the east phase over the Pacific ITCZ (Fig. 19a). Thus, while the DJF QBO enhancements over the Pacific

may be moderately associated with both hypothesized QBO mechanisms, the east phase Atlantic ITCZ signal may only be attributed to QBO modulation of tropopause height.

Unlike the SPCZ convective rainfall patterns, the JJA and SON SPCZ QBO stratiform rainfall variations extend beyond 10°S (Figs. 16c and 16d). Although magnitudes are weak, the SPCZ exhibits a west phase enhancement of stratiform rainfall. Poleward of 10°S, these regions of weak west phase enhancement correspond with the decrease of cross-tropopause shear (Figs. 18c and 18d) and tropopause temperatures (Figs. 19c and 19d) during the west phase.

Correlations between stratiform rainfall and QBO modulation of cross-tropopause shear and tropopause temperature for each season and region are given in Tables 5 and 6. The relationship between cross-tropopause shear and stratiform rainfall is generally weak as is indicated by Table 5. However, moderate positive correlations over the Indian Ocean and W. Pacific during SON and South America and the Atlantic during MAM suggest a modest association between the increase of stratiform rain and stronger cross-tropopause shear. The Maritime continent correlations generally suggest the opposite. Table 6 also suggests an overall weak relationship between stratiform rain and QBO variations in tropopause temperature. However, moderate negative correlations over the Maritime continent suggest that the enhancements in stratiform rainfall in this region can be associated with cooler tropopause temperatures.

4.3 The QBO's Influence on Convective Echo Top Height

The QBO's influence on DJF convective echo top heights is best seen in Africa, the Maritime continent, the north coast of Australia, and S. America (Fig. 17a). West minus east convective echo top height anomalies show the largest east phase enhancement to occur in Africa and north of Australia. Positive absolute 50-200 hPa shear values between 10°N and 10°S indicate cross-tropopause shear is weaker during the east phase (Fig. 18a). Therefore, the southern near-equatorial African and weak W. Pacific east phase signals are associated with QBO modulation through shear. Due to the increase of shear and temperatures during the west phase (Figs. 18a and 19a), the weak west phase signal over the Maritime continent is not associated with either hypothesized QBO mechanism. QBO modulation through shear does not account for the east phase maximum north of Australia as this area experiences a transition to stronger east phase shear; however, the decrease in temperature during the east phase is associated with an intense east phase increase of convective echo tops. The strong west phase signal in S. America materializes in an area of decreasing cross-tropopause shear and tropopause temperatures during the west phase of the QBO.

Similar to the convective and stratiform rainfall anomalies, convective echo top anomalies switch signs between DJF and MAM in many regions of the tropics (Fig. 17b); however, the MAM patterns are somewhat noisier. The largest QBO enhancements occur over southern India and Mexico. While cross-tropopause shear in Mexico is stronger during the east phase, positive 50-200 hPa shear anomalies indicate stronger west phase shear in near-equatorial Africa, India, and the Maritime continent (Fig. 18b).

Positive tropopause temperature anomalies indicate warmer temperatures during the west phase throughout Africa and the Maritime continent. However, negative anomalies across Mexico show that tropopause temperatures increase during the east phase (Fig. 19b). Thus, QBO variations in cross-tropopause shear and tropopause temperatures cannot account for the west phase increase of convective echo tops in near-equatorial Africa, India, and the Maritime continent. The increase in the amount of convective echo tops in Mexico is associated with QBO modulation through height and shear.

Following the seasonal migration of rain, JJA convective echo top anomalies shift north (Fig. 17c). The west minus east JJA convective echo top map shows a QBO west phase signal in the Congo, South China Sea, and E. Pacific. Enhancement in the QBO's east phase occurs over India and the Maritime continent. Cross-tropopause shear anomalies are positive in near-equatorial Africa, the Indian Ocean, the Maritime continent, and the Amazon basin (Fig. 18c). Contrary to expectations, the west phase increase of convective echo tops in Africa and the E. Pacific occurs in an area of stronger west phase shear. East phase enhancements in southern India, the Maritime continent, and northern S. America correspond to weaker east phase shear. Tropopause temperature difference anomalies indicate a lower tropopause during the west phase throughout Fig. 19c. Thus, the east phase signals in India and the Maritime continent are associated with the decrease in tropopause temperatures during the east phase of the QBO.

Figure 17d shows a relatively noisy map of negative and positive west minus east convective echo top counts during SON, although a weak east phase enhancement is

present over the majority Maritime continent, with the exception of a moderate west phase enhancement over Sumatra. Absolute 50-200 hPa shear and tropopause temperature anomalies increase during the west phase over the Maritime continent (Fig. 18d and 19d). Therefore, the east phase signals throughout the Maritime continent may be attributed to QBO modulation through shear and height.

Correlations between convective echo top and QBO modulation of shear and temperature are given in Tables 7 and 8. The Maritime continent consistently shows relatively moderate negative correlations suggesting a modest relationship between convective echo top height variations and QBO modulation of shear and temperatures. The Indian Ocean, W. Pacific, and E. Pacific also illustrate moderate correlations, although the correlations can be both negative and positive suggesting a complicated relationship between deep convective echo top counts and shear and tropopause temperatures. Similar to convective and stratiform rain correlations, weak regional convective echo top correlations suggest other factors overpower the QBO's influence in modulating tropical deep convection via cross-tropopause shear and tropopause heights.

4.4 PR Convective Responses and Variations in Cross-tropopause Shear and Tropopause Temperatures

Our exploration of the basic relationship between deep convective responses and cross-tropopause shear and tropopause temperature variations extends to convective and stratiform rainfall and convective echo top heights. Correlation coefficients between monthly values of PR data, i.e., convective and stratiform rainfall and convective echo

top heights, and monthly values of cross-tropopause shear and tropopause temperatures are mapped out in Figs. 20-25. Negative (positive) correlations indicate an increase in the deep convective property when cross-tropopause shear is decreasing (increasing) and the tropopause is higher/colder (lower/warmer).

Figure 20 maps the correlation coefficients between convective rainfall and cross-tropopause shear. With the exception of SON, negative correlations in the Indian Ocean indicate a weak increase in convective rainfall with decreasing cross-tropopause shear. Sparse and weak correlations in the Maritime continent during DJF suggest that variations in cross-tropopause shear do not affect convective rainfall. However, MAM correlation values of 0.4 indicate that the increase in cross-tropopause shear may be linked to an increase in convective rainfall in the Maritime continent. Correlation values across the Maritime continent transition from positive in MAM to negative in JJA and SON; thus, the decrease in 50-200 hPa shear is associated with an increase in convective rain. With the exception of DJF, Fig. 20 indicates that convective rainfall in the W. Pacific moderately increases when cross-tropopause shear decreases. Low positive DJF correlations in the center of the SPCZ indicate a weak enhancement of convective rainfall in an area of increasing shear. However, negative correlations along the SPCZ boundary show an increase in convective rainfall with weakening cross-tropopause shear. In general, the SPCZ during MAM exhibits a modest enhancement of convective rainfall with weaker cross-tropopause shear. It is noted that the relationship between convective rainfall and cross-tropopause shear variations during JJA and SON is not seen past 10°S. Correlations in the Pacific ITCZ generally show that a decrease in cross-

tropopause shear is associated with an increase in convective rain. Convective rainfall in the E. Pacific and Atlantic both show their strongest relationship with cross-tropopause shear during MAM. While E. Pacific convective rainfall weakly increases with decreasing shear, convective rainfall in the Atlantic moderately increases with increasing cross-tropopause shear.

Tropopause temperature and convective rainfall correlations are mapped in Fig. 21. Figure 21a shows that the strongest modification by tropopause temperature variations in the Indian Ocean occurs during DJF. In general, the Maritime continent and W. Pacific experience a moderate increase in convective rainfall when tropopause temperatures become colder. A patchwork of weak negative and positive correlations during DJF and MAM in the SPCZ shows a weak relationship between convective rainfall and tropopause temperature variations. SPCZ convective rainfall is weakly enhanced when tropopause temperatures are lower during JJA and SON. Contrary to the relationships with cross-tropopause shear, tropopause temperature correlations in the ITCZ show more positive values in DJF and JJA; thus, ITCZ convective rainfall is possibly weakly enhanced by warmer tropopause temperatures. It is noted that a large area in S. America during SON experiences a weak enhancement of convective rainfall when tropopause temperatures are warmer. Unlike Fig. 20, the E. Pacific and Atlantic begin to show a year round signal in tropopause temperature and convective rainfall correlations. Therefore, variations in tropopause temperatures in the E. Pacific and Atlantic may have a stronger influence on convective rainfall than cross-tropopause shear.

Correlations between stratiform rainfall and variations in cross-tropopause shear are mapped in Fig. 22 and are generally similar to the convective rain correlations in Fig. 20. However, the following are notable differences. DJF correlations indicate a weak-to-moderate enhancement of stratiform rainfall with decreasing cross-tropopause shear over the Pacific ITCZ (Fig. 22a). During JJA, enhancements of stratiform rainfall over the off-equator SPCZ and north northwest Pacific are weakly associated with stronger cross-tropopause shear (Fig. 22c). SON correlations indicate stratiform rain over the off-equator SPCZ and over southeastern S. America increases when cross-tropopause shear is increasing (Fig. 22d). Figure 23 maps the correlations between stratiform rain and tropopause temperature variations and, again, are generally similar to the convective correlations in Fig. 21 with the exception of regions near 20°N and S in the Pacific basin. It appears that convective and stratiform rain have similar relationships to cross-tropopause shear and tropopause heights across most of the Tropics at monthly time scales.

In general, the 50-200 hPa shear and convective echo top correlations in Fig. 24 show a weak relationship between the number of convective cells penetrating 200 hPa and cross-tropopause shear variations. DJF convective echo top heights in near-equatorial Africa weakly increase when cross-tropopause shear decreases. Some of the larger islands in the Maritime continent and the Amazon basin experience an increase in convective echo top heights when cross-tropopause shear is strengthening. Decreasing 50-200 hPa shear in MAM is associated with a general increase of deep convective echo tops in the Indian Ocean, SPCZ, and southern regions of S. America, while the opposite

is case over northern Brazil and the Atlantic ITCZ (Fig. 24b). While increasing shear in JJA is coincident with an increase in convective echo tops over Africa and Mexico, convective echo tops across the Maritime continent, W. Pacific, E. Pacific, and northern S. America increase with decreasing shear (Fig. 24c). SON exhibits an increase in convective echo tops in the presence of increasing cross-tropopause shear in Africa and the Maritime continent and a decrease in convective echo tops over much of the Pacific (Fig. 24d).

Convective echo top height counts and tropopause temperature correlations show a stronger relationship than the shear correlations (Fig. 25). Negative correlations over Africa, the W. Pacific, and southern S. America during DJF suggest convective echo top heights increase when tropopause temperatures are colder (Fig. 25a). Although slightly weaker, MAM negative correlations in the Maritime continent, W. Pacific, E. Pacific, and S. America also exhibit an increase in convective echo tops when tropopause temperatures decrease (Fig. 25b). Correlations in Africa and the Maritime continent switch from predominantly negative values in MAM to predominantly positive values in JJA; thus, warmer temperatures in JJA are linked with a weak increase in the amount of convective echo tops penetrating higher altitudes (Fig. 25c). However, India, Thailand, and Central America experience an increase in convective echo tops when tropopause temperatures are lower during JJA. Weak SON negative correlations north of the Maritime continent and over Central America suggest a weak increase in convective echo tops with decreased tropopause temperatures (Fig. 24d). Convective echo tops in

the Amazon basin weakly increased with warmer tropopause temperatures as is indicated by the low positive values during SON.

5. SUMMARY AND CONCLUSIONS

Eight years (1998-2005) of LIS flash densities and ten years (1998-2007) of TRMM PR data were used to examine the QBO's relationship to deep tropical convection. Using TRMM 2A23 and 2A25 V6 PR orbital data, ten years of monthly histograms containing longitude, latitude, height, corrected reflectivity, and echo top height were constructed. West and east phase months of the QBO were defined by a 50-70 hPa shear index. The LIS (PR) period contained three (four) full QBO cycles. Flash densities, convective rainfall, stratiform rainfall, and convective echo top heights were partitioned by QBO phase.

Zonal mean anomalies averaged for the QBO west and east phase were calculated for each convective property and corresponding cross-tropopause shear and tropopause temperatures. Flash density and convective and stratiform rainfall zonal anomalies revealed QBO east and west phase signals symmetric about the equator with maximum anomalies near the equator. However, QBO signal symmetric about the equator was not present in convective echo top anomalies. Instead, convective echo top anomalies reached a maximum in the Northern Hemisphere and decreased closer to the equator. Flash density zonal monthly mean anomalies are inconsistent with the hypothesis that a decrease in cross-tropopause shear and/or tropopause temperature will deepen convection and thus lightning production. However, convective and stratiform rainfall east phase zonal mean anomalies were positive about the equator indicating increased convection with weak cross-tropopause shear and a higher tropopause. Comparison of flash densities and zonal mean anomalies indicates variations in lightning

during the QBO range from 0.5%-2.5%. The QBO accounts for 4% of convective rainfall, 6% of stratiform rainfall, and 12% of convective echo top variations.

West minus east seasonal 50-200 hPa anomalies indicate a year round band of stronger west phase shear that begins in equatorial Africa and continues into the W. Pacific. Depending on the season, the E. Pacific and Amazon basin also generally experience an increase in shear during the west phase. With the exception of DJF, zonal and seasonal monthly mean tropopause temperature east phase anomalies indicate a higher/colder than normal tropopause throughout the Tropics.

Longitudinal and seasonal variations in flash densities were addressed by mapping west minus east LIS monthly mean anomalies. The resulting map showed distinct lightning QBO signals. Contrary to expectations, west minus east DJF flash densities show large areas of west phase enhancement in near-equatorial regions, especially over the Maritime continent. QBO near-equatorial flash density anomalies generally transitioned from a west phase signal in DJF to an east phase signal in MAM. JJA and SON LIS difference maps show a west phase enhancement of near-equatorial flash densities. While flash density and QBO modulation of cross-tropopause shear and tropopause temperature correlations are generally weak, negative correlations in India consistently show the strongest relationship between lightning production and the hypothesized QBO mechanisms. Positive correlations between flash densities and cross-tropopause shear and tropopause temperatures suggest that the hypothesized QBO mechanisms have a relationship opposite of that expected during particular seasons and regions, e.g., Africa during JJA and the Maritime Continent/Australia during JJA and

SON. In these instances, it is possible that other factors such as the monsoon overwhelm the QBO's influence on lightning production.

Unlike the west minus east QBO LIS anomalies, west minus east convective and stratiform rainfall anomalies illustrate a robust QBO signal over the oceans. In general, convective and stratiform rain QBO variations are similar. During DJF, the Maritime continent, W. Pacific, and E. Pacific and Atlantic ITCZs experience a moderate east phase enhancement of deep convective rainfall. The opposite is true over the Indian Ocean. Convective and stratiform rainfall anomalies across the Maritime continent, W. Pacific, and E. Pacific and Atlantic ITCZs transition from a robust east phase signal in DJF to a moderate west phase signal in MAM. However, the opposite transition occurs in the Indian Ocean. A Tropics-wide pattern similar to MAM is maintained in JJA, and then reverses again in SON to a QBO pattern more similar to DJF. Correlations suggest that the strongest relationships between convective rainfall and QBO variations in cross-tropopause shear and tropopause temperatures are over the Maritime continent (negative values predominate), E. Pacific (negative shear and positive temperature values predominate), and Atlantic (both negative and positive values predominate depending on season and mechanism). Correlations between stratiform rainfall and the QBO modulation of shear and height are strongest over the Maritime continent (negative) and Atlantic (positive).

Convective echo top anomalies experience a moderate east phase enhancement in Africa and north of Australia during DJF. The opposite is true over the Maritime continent and S. America. The MAM convective echo top anomaly pattern is somewhat

noisier, although hot spots of west phase enhancement occur over southern India and Mexico and the far E. Pacific. The amount of JJA convective echo tops penetrating 200 hPa increases during the west phase in near-equatorial Africa and the E. Pacific and weakly increases during the east phase in the Maritime continent. However, the strongest JJA convective echo top QBO signal occurs over the Indian subcontinent during the east phase. With the exception of Sumatra, the Maritime continent continues to show an east phase enhancement of convective echo tops during SON. Otherwise the SON pattern is fairly noisy. Compared to deep convective rainfall, relationships between convective echo tops and QBO variations in cross-tropopause shear and tropopause temperature are generally weaker. Correlations suggest that a decrease in cross-tropopause shear and tropopause temperatures during the QBO has the strongest association with an increase in convective echo tops > 12 km over the Maritime continent.

Correlations between monthly values of 50-200 hPa shear and flash densities, rainfall, and convective echo tops are generally weak suggesting that the increase or decrease of deep convective properties is weakly associated with variations in cross-tropopause shear. The decrease of shear during DJF is linked to the weak enhancement of flash densities over near-equatorial Africa, Australia, and the Amazon and to the weak enhancement of rainfall over the Indian Ocean. Flash densities over S. America and rainfall and convective echo tops over the SPCZ have a modest relationship with decreasing cross-tropopause shear during MAM. However, the Maritime continent and Atlantic ITCZ exhibit a moderate increase in rainfall with increasing cross-tropopause shear. For the most part, JJA correlations indicate an increase in flash densities when

shear is increasing. In addition, weaker cross-tropopause shear is weakly associated with rainfall over the Indian Ocean and Maritime continent and convective echo tops over the Maritime continent and S. America. Generally, SON correlations indicate a weak relationship between variations in cross-tropopause shear and deep convective properties.

Compared to cross-tropopause shear relationships, tropopause temperature correlations indicate a modest association between deep convective properties and variations in tropopause height. DJF correlations suggest a modest relationship between a higher/colder tropopause and flash densities over the Maritime continent and Brazil, rainfall over the Indian Ocean, Maritime continent, and W. Pacific, and convective echo tops over near-equatorial Africa and the Maritime continent. While warmer tropopause temperatures in MAM are associated with an enhancement of flash densities over near-equatorial Africa and northwestern S. America, rainfall amounts over the Maritime continent, W. Pacific, and E. Pacific and convective echo tops over the Maritime continent and S. America increase when tropopause temperatures are cooler. Flash density and deep convective rainfall variations during JJA are associated with an increase in tropopause temperatures. However, convective echo tops are enhanced when tropopause temperatures are cooling. With the exception of the Maritime continent, SON correlations indicate a modest relationship between the enhancement of flash densities and decreasing tropopause temperatures. In addition, rainfall over the Maritime continent, W. Pacific, and ITCZ and convective echo tops over the Maritime continent weakly increase with cooler tropopause temperatures. It is noted that correlations

indicate that deep convective properties over the Maritime continent consistently show a strong relationship with cross-tropopause shear and tropopause temperature variations.

To conclude, a QBO signal is present in lightning, rainfall, and the number of deep convective cells when analyzing zonal and seasonal monthly mean anomalies. In parts of the Tropics, QBO variations of flash densities, convective and stratiform rainfall, and convective echo tops show a physically consistent relationship with QBO variations in cross-tropopause shear and tropopause height, while in other parts of the Tropics relationships between the deep convective properties and hypothesized QBO mechanisms are inconsistent. The generally weak correlations presented in Tables 1-8 sustain the variable relationship between the QBO and deep convection that is seen in observations. Thus, other factors that influence convective activity must be overwhelming the QBO's effects on tropical deep convection.

To further the work done in this study, longer TRMM LIS and PR records are needed. Future work can be done in determining how QBO variations in cross-tropopause shear and tropopause temperatures affect stratiform rain fraction. In addition, future studies should focus on separating the ENSO signal from the QBO signal in convection. Even for a particular season or region, an established relationship between the QBO and tropical deep convection could be useful in providing forecasts for tropical rainfall.

REFERENCES

Andrews, D. G., and J. R. Holton, and C. B. Leovy, 1987: *Middle Atmosphere Dynamics*, 489 pp., Academic Press, San Diego, Calif.

Awaka, J., T. Iguchi, H. Kumagai, and K. Okamoto, 1997: Rain type classification algorithm for TRMM precipitation radar, *Proc. IEEE 1997 Int. Geoscience and Remote Sensing Symp.*, 1633-1635.

Baldwin, M. P., and Coauthors, 2001: The Quasi-Biennial Oscillation. *Rev. Geophys.*, **39**, 179-229.

Bretherton, F. P., 1969: Momentum transport by gravity waves. *Q. J. R. Meteorol. Soc.*, **95**, 213-243.

Christian, H. J., and Coauthors, 1999: The Lightning Imaging Sensor. *Proceedings of the 11th International Conference on Atmospheric Electricity*, Guntersville, Alabama, 746-749. [Available online at http://thunder.msfc.nasa.gov/bookshelf/pubs/LIS_ICAE99_Print.pdf]

Christian, H. J., R. J. Blakeslee, S. J. Goodman, and D. M. Mach, 2000: Algorithm Theoretical Basis Document (ATBD) for the Lightning Imaging Sensor (LIS). 1-53. [Available online at http://eospso.gsfc.nasa.gov/eos_homepage/for_scientists/atbd/docs/LIS/atbd-lis-01.pdf]

Collimore, C. C. M. H. Hitchman, and D. W. Martin, 1998: Is there a quasi-biennial oscillation in tropical deep convection? *Geophys. Res. Lett.*, **25**, 333-336.

Collimore, C. C., and Coauthors, 2003: On the relationship between the QBO and tropical deep convection. *J. Climate*, **16**, 2552-2568.

Dunkerton, T. J., 1997: The role of gravity-waves in the quasi-biennial oscillation. *J. Geophys. Res.*, **102**, 26,053-26,076.

Gagin, A., D. Rosenfeld, and R.E. Lopez, 1985: The relationship between height and precipitation characteristics of summertime convective cells in South Florida. *J. Atmos. Sci.*, **42**, 84-94.

Gray, W. M., J. D. Schaeffer, and J. A. Knaff, 1992: Influence of the stratospheric QBO on ENSO variability. *J. Meteor. Soc. Japan,* **70**, 975-995.

Hamilton, K., and Coauthors, 2004: Longitudinal variation of the stratospheric Quasi-Biennial Oscillation. *J. Atmos. Sci.*, **61**, 383-402.

Houze, R.A. 1981: Structures of atmospheric precipitation systems – a global survey, *Radio Science*, **16**, 671-689.

Huesmann, A. S., and M. H. Hitchman, 2001: The stratospheric quasi-biennial oscillation in the NCEP reanalysis: climatological structures. *J. Geophys. Res*., **106**, 11,859-11,874.

Iguchi, T., T. Kozu, R. Meneghini, J. Awaka, and K. Okamoto, 2000: Rain-profiling algorithm for the TRMM precipitation radar. *J. Appl. Meteor.*, **39**, 2038-2052.

Kalnay, E., and Coauthors, 1996: The NCEP/NCAR 40-year reanalysis project, *Bull. Amer. Meteor. Soc.*, **77**, 437-470.

Lindzen, R. S., and J. R. Holton, 1968: A theory of the Quasi-Biennial Oscillation. *J. Atmos. Sci.*, **25**, 1095-1107.

Mushtak, V. C., E. R. Williams, and D. J. Boccippio, 2005: Latitudinal variations in cloud base height and lightning parameters in the tropics. *Atmos. Res.*, **76**, 222-230.

Okamoto, K., and Coauthors, 2004: Tropical Rainfall Measuring Mission (TRMM) Precipitation Radar Algorithm Instruction Manual (version 1) for Version 6. 1-157. [Available online at http://eorc.jaxa.jp/TRMM/documents/PR_algorithm_product_information/pr_manual/pr_manual_v4.pdf]

Reed, R. J., W. J. Campbell, L. A. Rasmussen, and D.G. Rogers, 1961: Evidence of downward propagating annual wind reversal in the equatorial stratosphere. *J. Geophys. Res.*, **66**, 813-818.

Rosenfeld, D., and A. Gagin, 1989: Factors governing the total rainfall yield from continental convective clouds. *J. Appl. Meteor.*, **28**, 1015-1030.

Shimizu, S., and Coauthors, 2003: Validation analyses after the altitude change of TRMM. *Proc. SPIE*., **4894**, 9 pp.

Steiner, M., R. A. Houze, and S. Yuter, 1995: Climatological characterization of three-dimensional storm structure from operational radar and rain gauge data. *J. Appl. Meteor.*, **34**, 1978-2007.

Wallace, J. M., 1973: General circulation of the tropical lower stratosphere. *Rev. Geophys.*, **11**, 191-222.

Wallace, J. M., and V. E. Kousky, 1968: On the relation between Kelvin waves and the quasi-biennial oscillation. *J. Meteorol. Soc. Jpn.*, **46**, 496-502.

APPENDIX

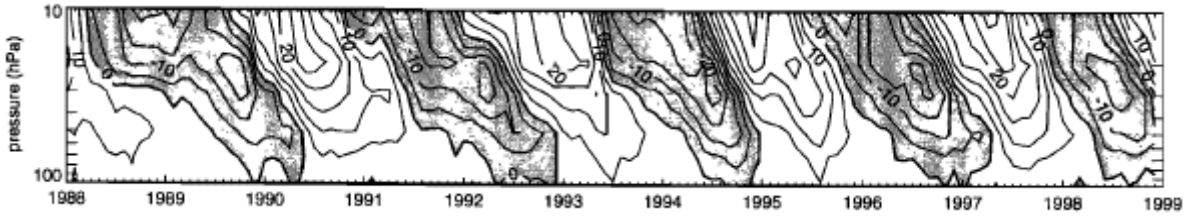

Figure 1: Zonally averaged anomalous equatorial zonal wind ($\overline{u_{eq}}$) as a function of time and pressure. F*rom Huesmann and Hitchman (2001).*

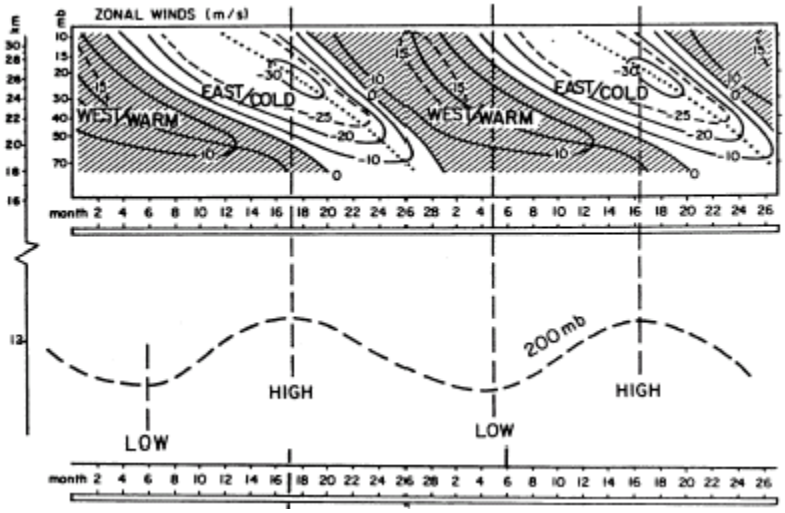

Figure 2: Top: Schematic rendering of the mean 28-29 month cycle of QBO zonal wind anomalies, beginning with the westerly (shaded) maximum and continuing through two cycles. Typical zonal wind speed anomalies at the equator are also shown in the top panel, expressed in m s^{-1}. Comparatively cold stratospheric temperature anomalies which typically accompany the QBO easterly shear and warm temperatures accompanying the westerly QBO are labeled as such. Bottom: Schematic rendering of the typical observed variations of 200mb height (dashed line) associated with the east and westerly shear phases. *From Gray et al. (1992).*

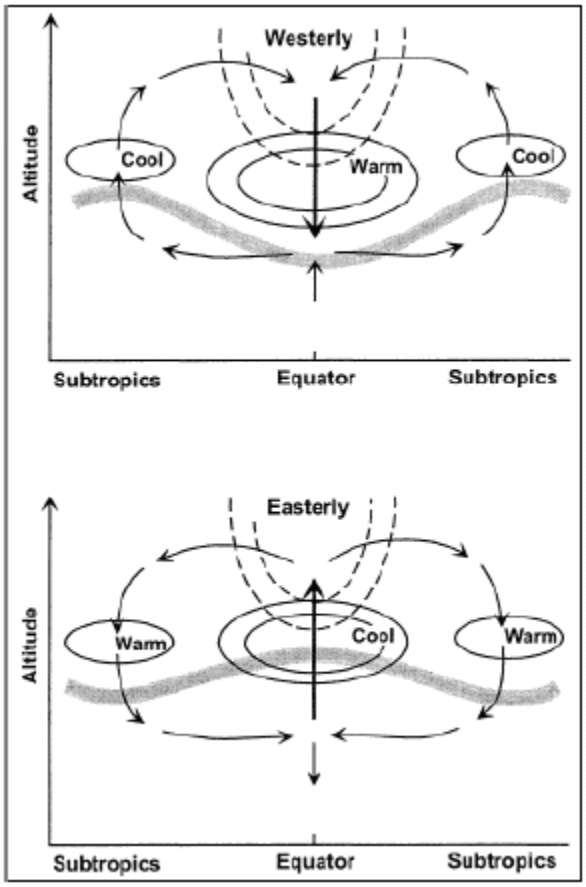

Figure 3: Schematic representation of QBO modulation through tropopause height during the west (top) and east (bottom) phase. The thick gray line represents the tropopause. From *Collimore et al.* [2003].

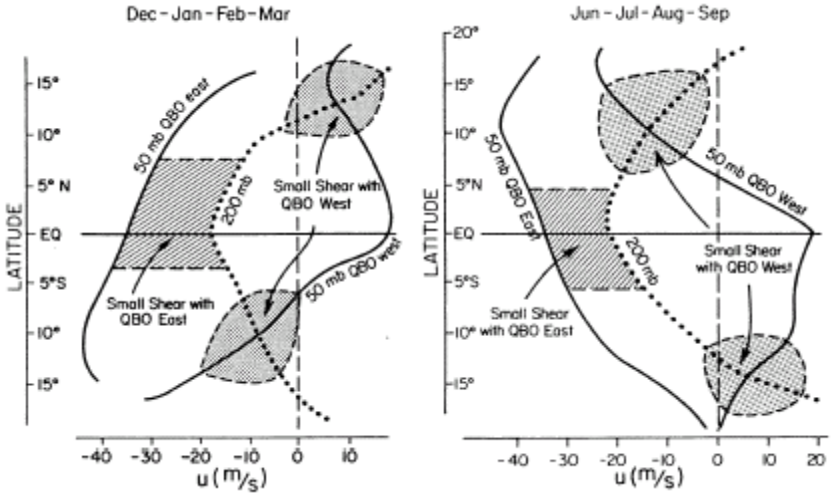

Figure 4: Absolute value of mean zonal wind speeds at 50mb (solid line) for December through March (left) and June through September (right) for typical east and west phase QBO periods. Zonal winds at 200mb are shown as dashed lines. The shaded areas enclose conditions of minimum 50-200mb zonal wind shear. *From Gray et al. (1992).*

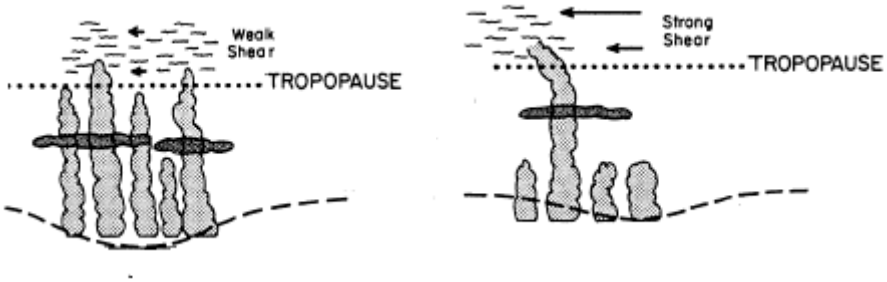

Figure 5: Schematic representation of weak (left) and strong (right) cross-tropopause shear effects on tropical convection. *Adapted from Gray et al. (1992).*

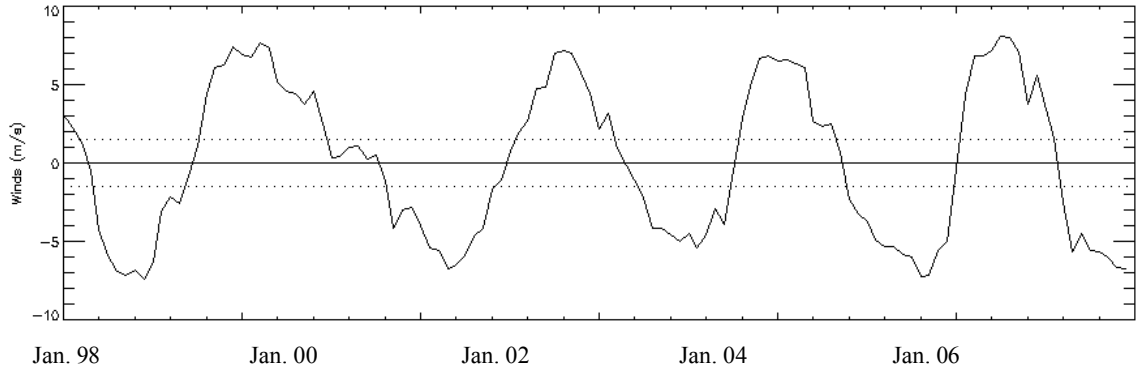

Figure 6: The 50-70 hPa QBO index for the 1998-2007. The dotted lines represent the ± 1.5 m s^{-1} threshold.

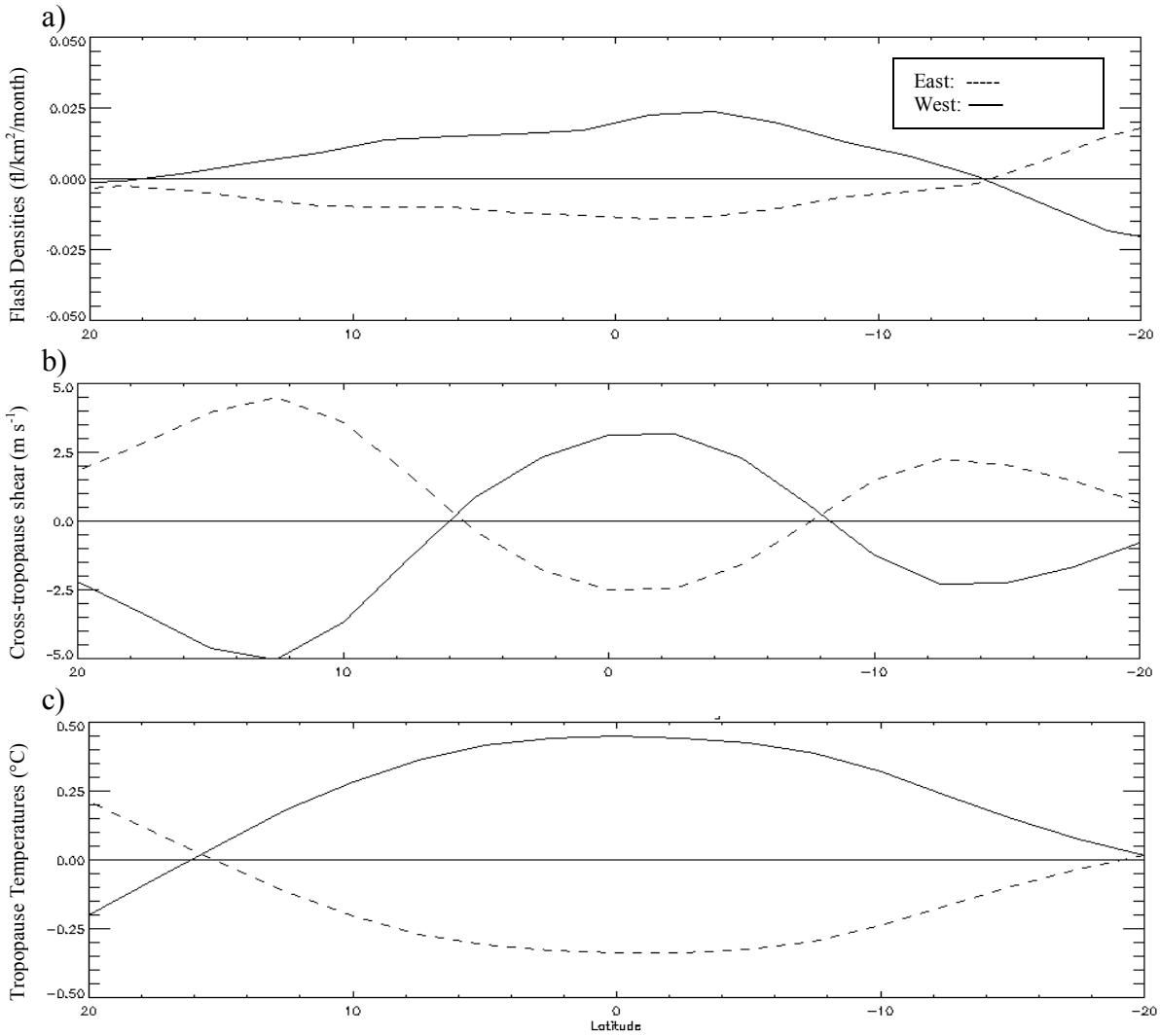

Figure 7: Zonal monthly mean anomalies averaged over the QBO east (dashed) and west (solid) phases for a) LIS flash density anomalies. Units are fl/km^2/month., b) absolute 50-200 hPa shear. Units are m s^{-1}., c) tropopause temperatures. Units are °C.

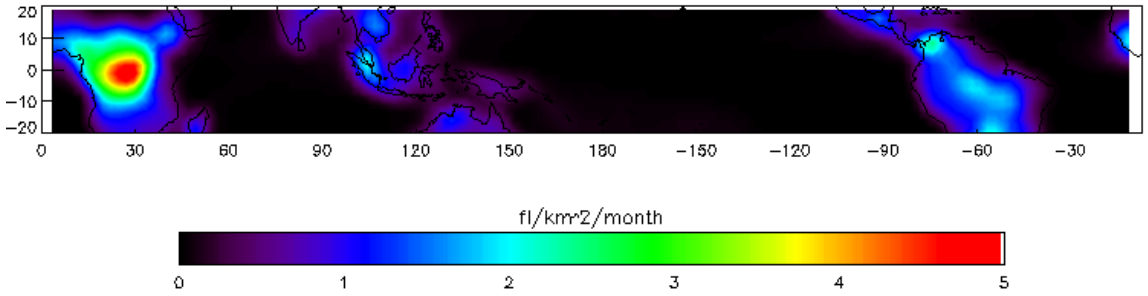

Figure 8: LIS flash density monthly means for 1998-2005. Units are fl/km^2/month.

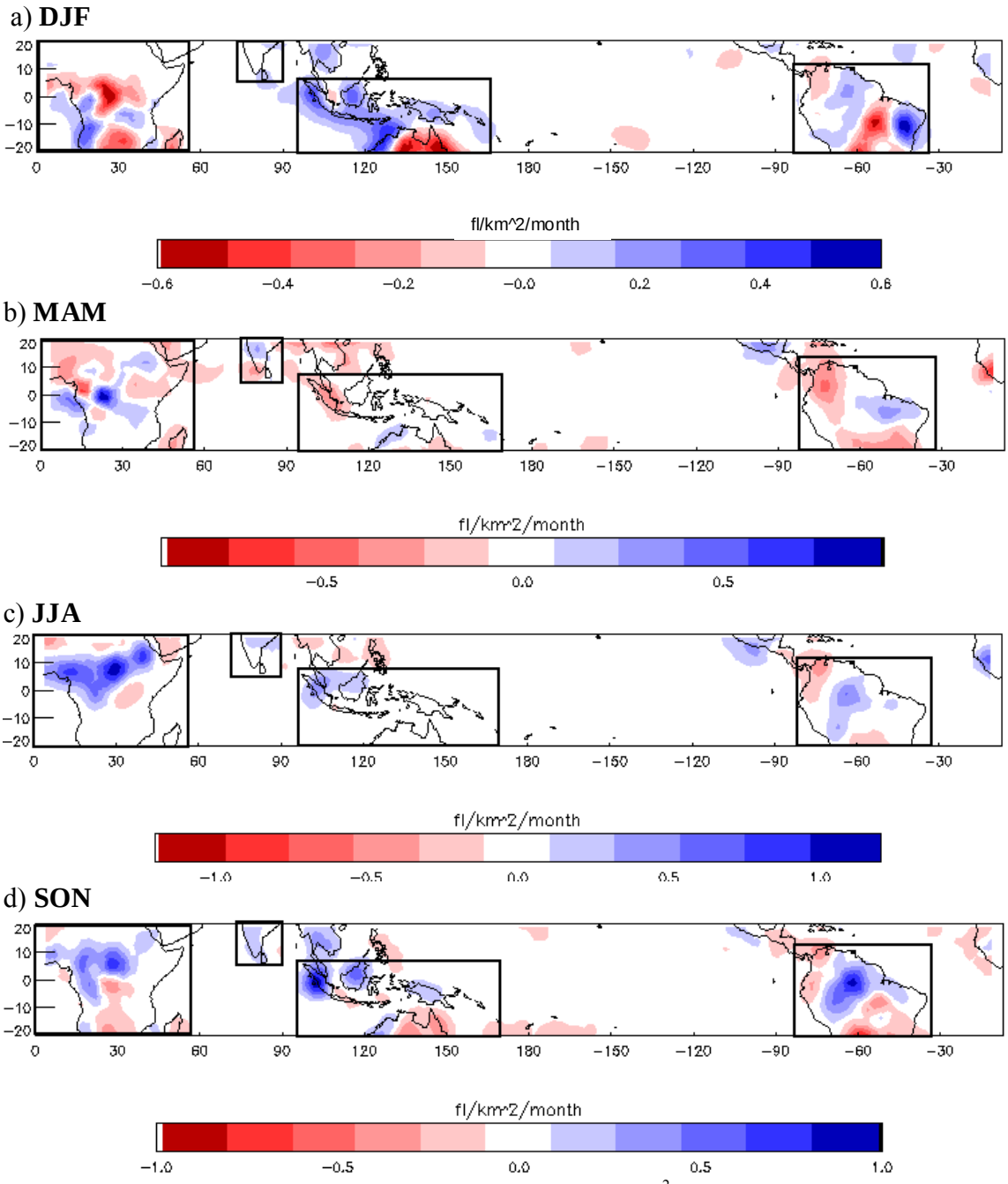

Figure 9: Mean anomalous QBO west minus east flash density (fl/km^2/month) maps for a) DJF, b) MAM, c) JJA, and d) SON. Red (blue) represents an increase in flash densities during the east (west) phase.

a) **DJF**

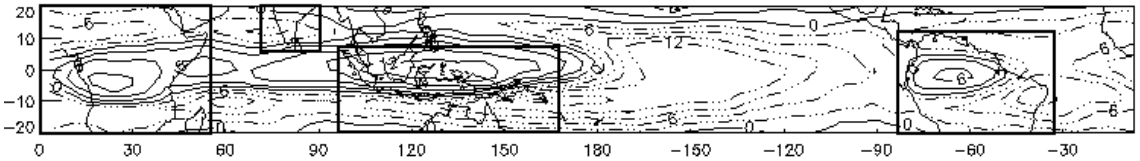

b) **MAM**

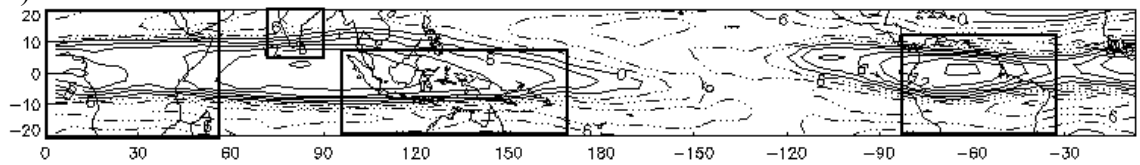

c) **JJA**

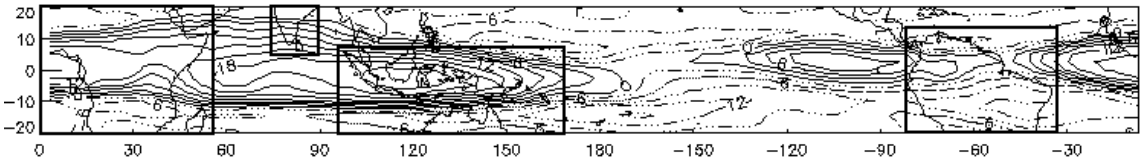

d) **SON**

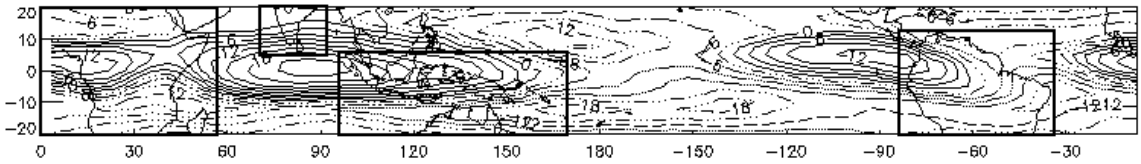

Figure 10: Mean anomalous west minus east absolute 50-200 hPa shear (m s^{-1}) maps for a) DJF, b) MAM, c) JJA, and d) SON. East (west) phase values are represented by dashed dotted (solid) lines.

a) **DJF**

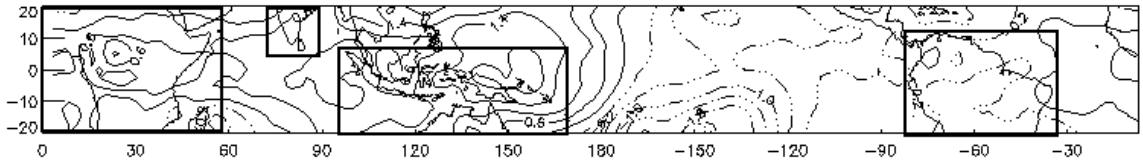

b) **MAM**

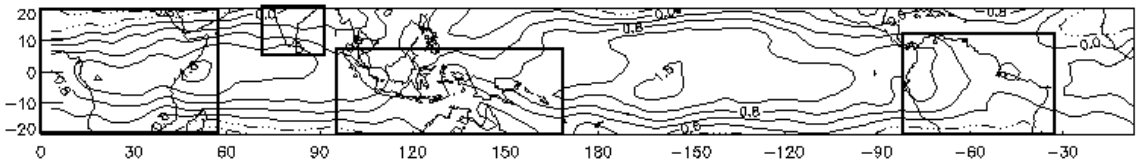

c) **JJA**

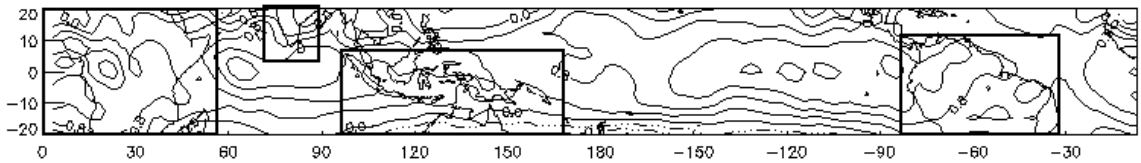

d) **SON**

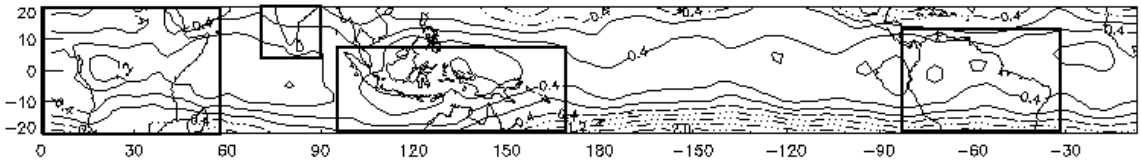

Figure 11: Mean anomalous west minus east temperature (°C) maps for a) DJF, b) MAM, c) JJA, and d) SON. East (west) phase values are represented by dashed dotted (solid) lines.

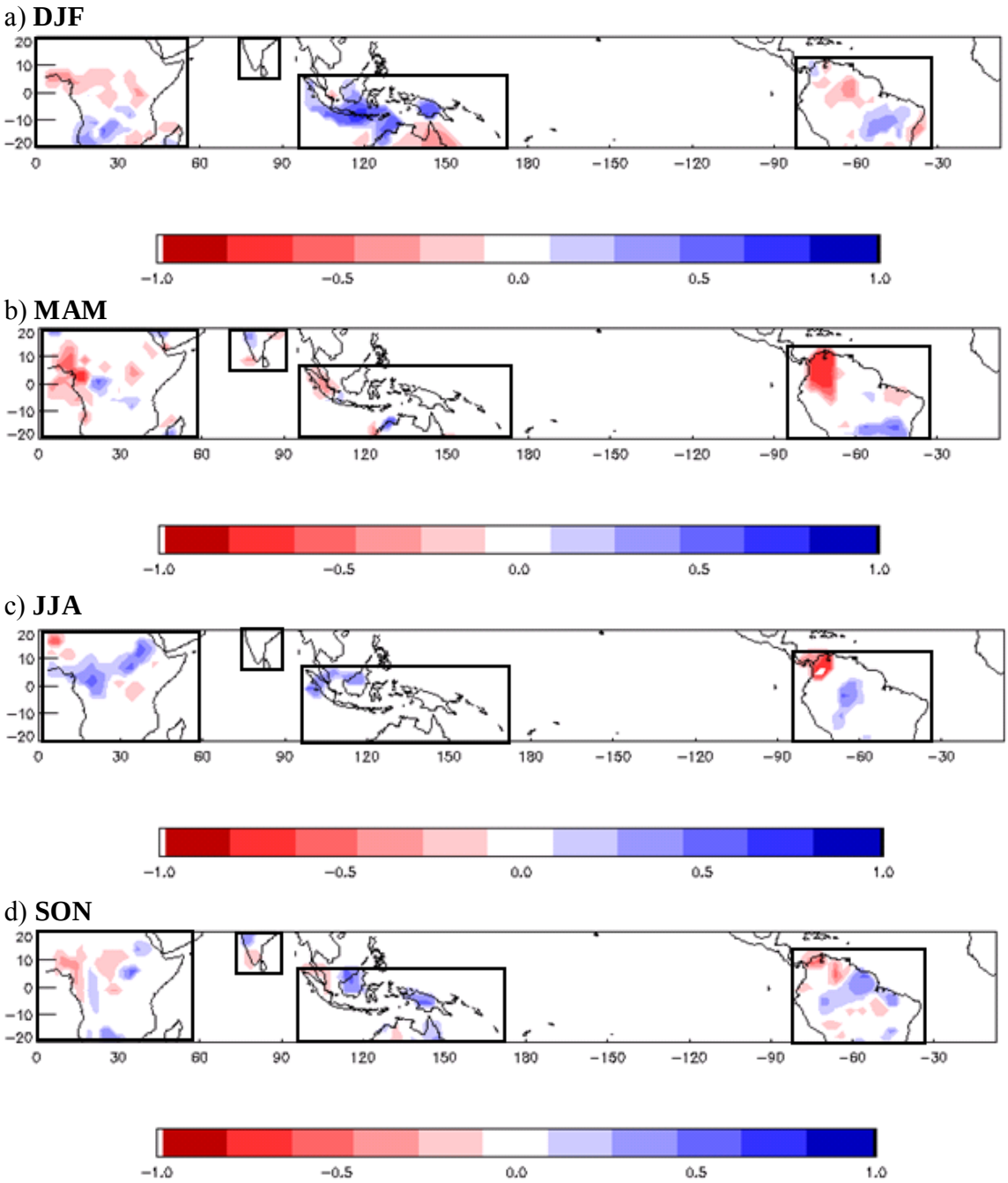

Figure 12: Correlation coefficients between monthly means of anomalous flash densities and anomalous QBO modulation of absolute 50-200 hPa shear during a) DJF, b) MAM, c) JJA, and d) SON. Red (blue) represents negative (positive) correlations.

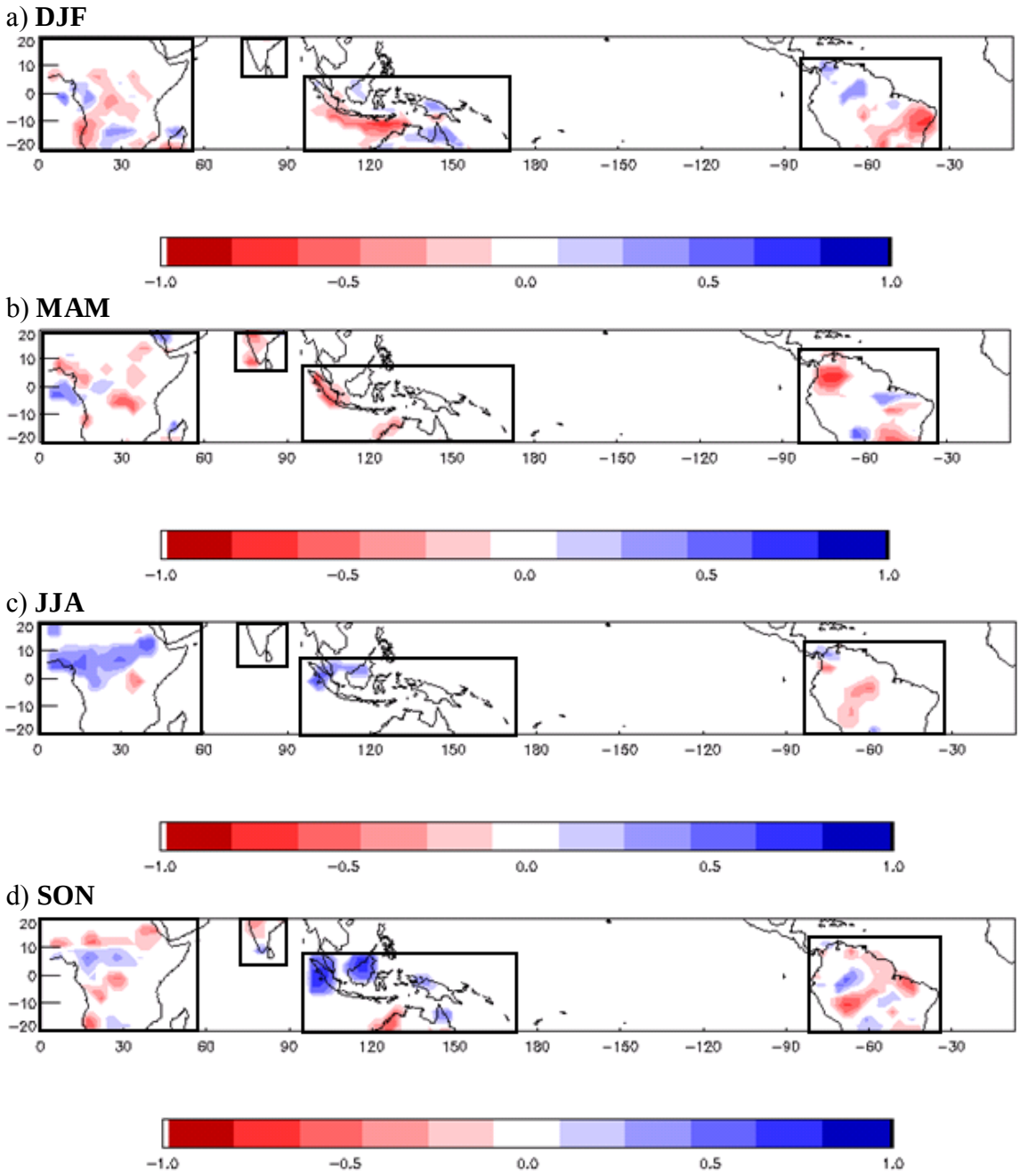

Figure 13: Correlation coefficients between monthly means of anomalous flash densities and anomalous tropopause temperatures during a) DJF, b) MAM, c) JJA, and d) SON. Red (blue) represents negative (positive) correlations.

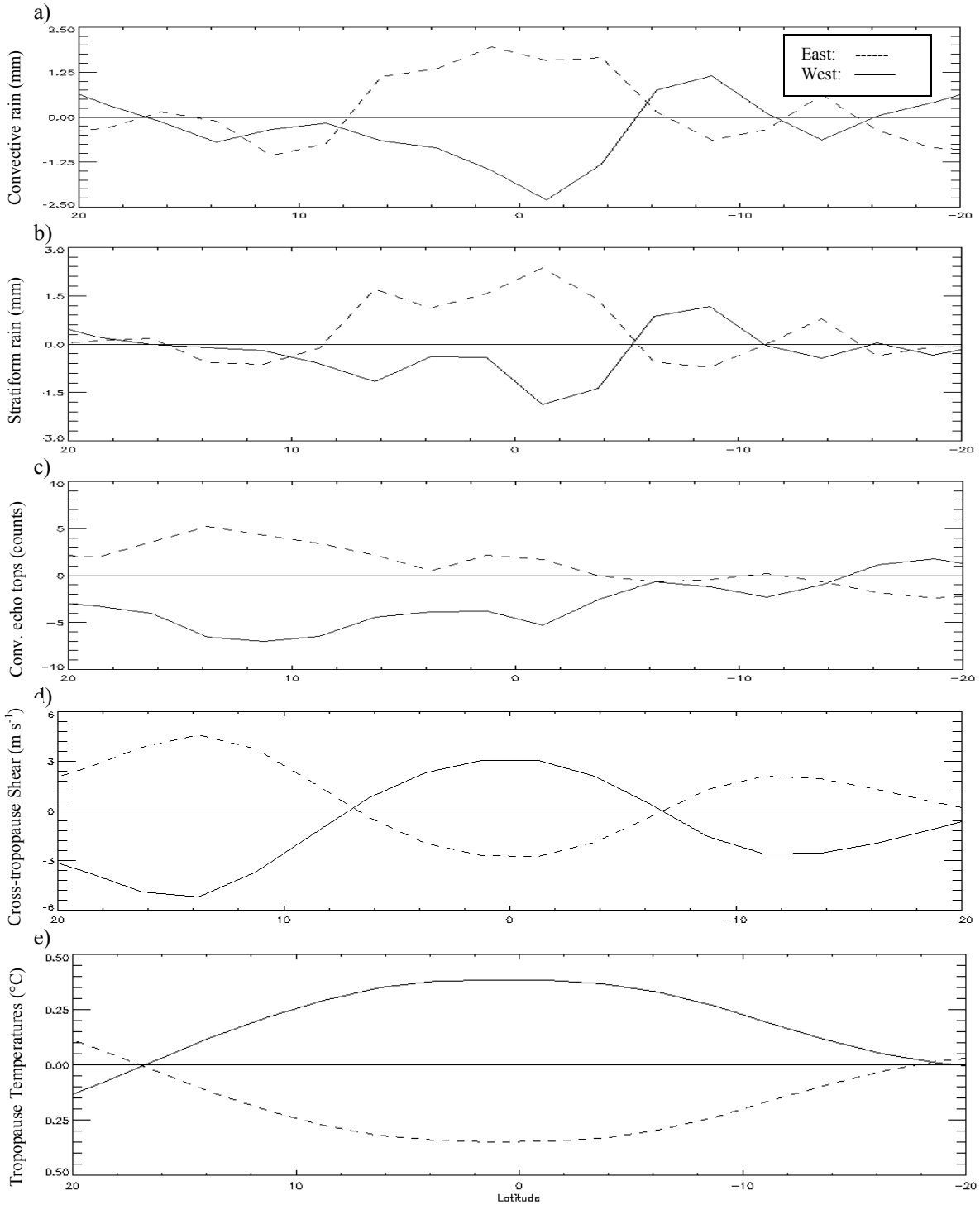

Figure 14: Zonal monthly mean anomalies for a) convective rainfall (mm), b) stratiform rainfall (mm), c) convective echo top heights between 12 km-20 km (counts), d) absolute 50-200 hPa shear (m s^{-1}), and d) tropopause temperatures (°C). The east (west) phase is denoted by the dashed (solid) line.

a) **DJF**

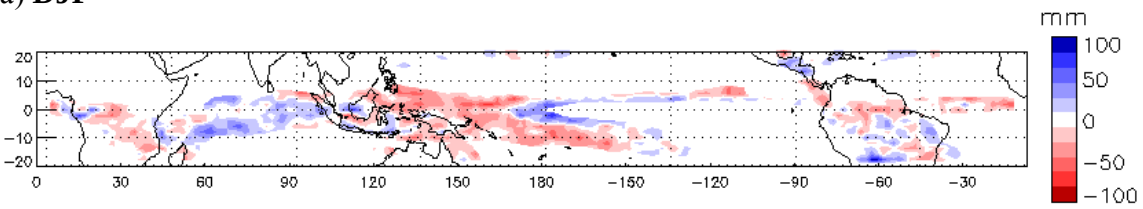

b) **MAM**

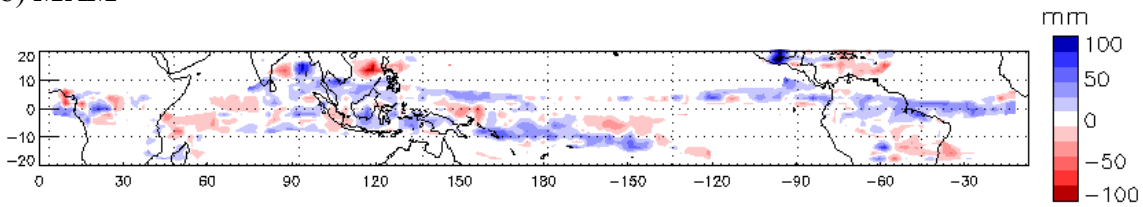

c) **JJA**

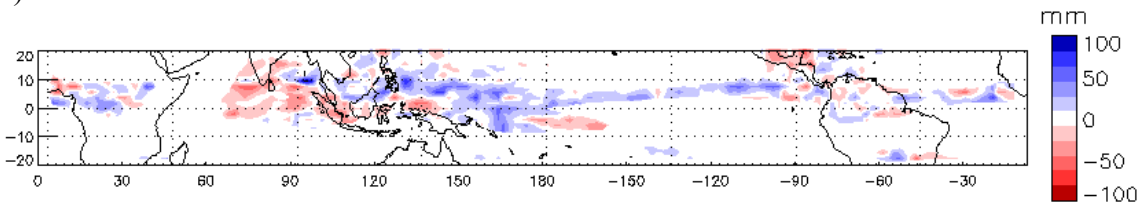

d) **SON**

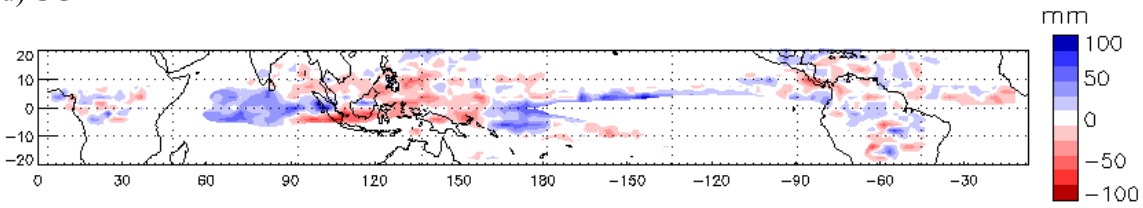

Figure 15: Monthly mean anomalous QBO west minus east convective rainfall (mm) maps for a) DJF, b) MAM, c) JJA, and d) SON. Red (blue) represents an increase in convective rainfall amounts during the east (west) phase.

a) **DJF**

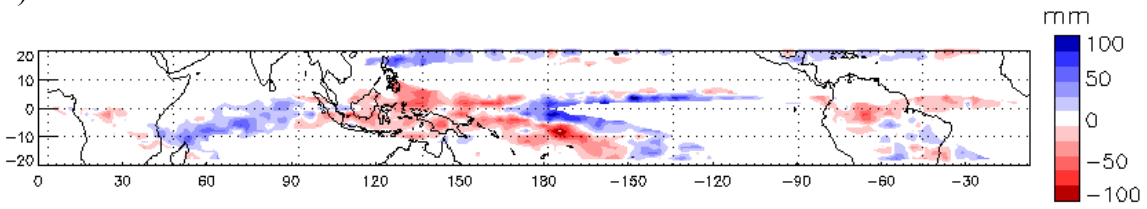

b) **MAM**

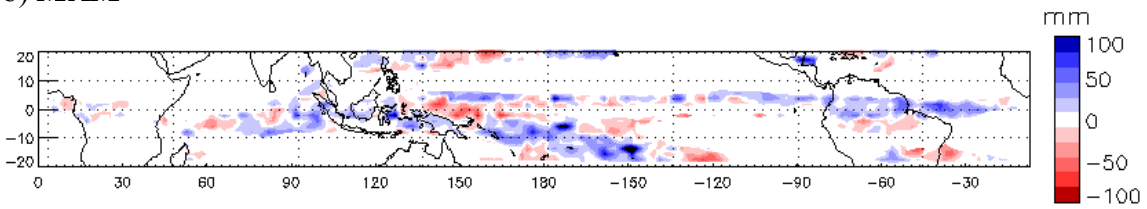

c) **JJA**

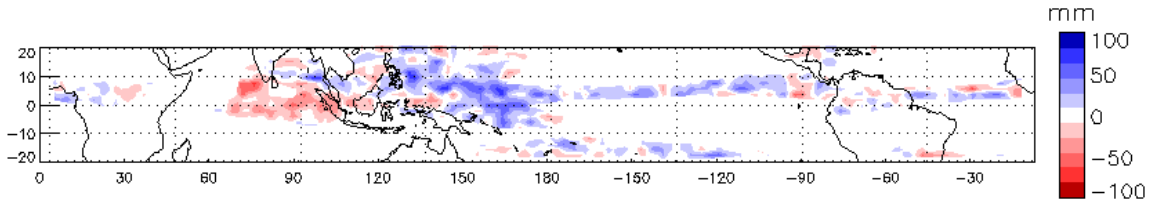

d) **SON**

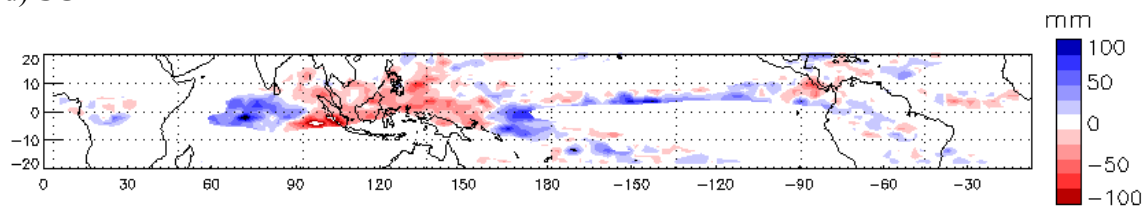

Figure 16: Monthly mean anomalous QBO west minus east stratiform rainfall (mm) maps for a) DJF, b) MAM, c) JJA, and d) SON. Red (blue) represents an increase in stratiform rainfall during the east (west) phase.

a) **DJF**

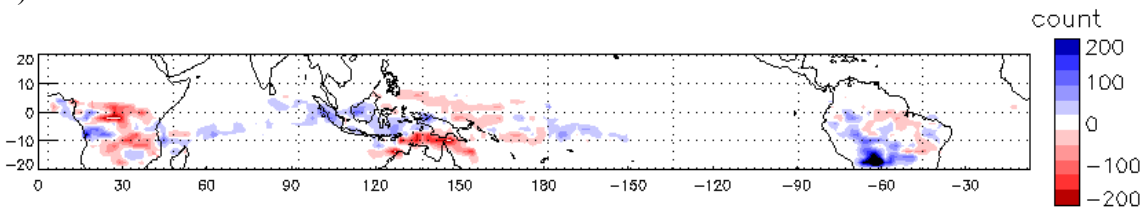

b) **MAM**

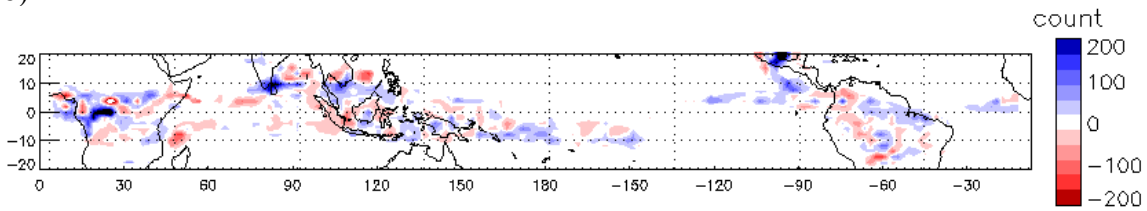

c) **JJA**

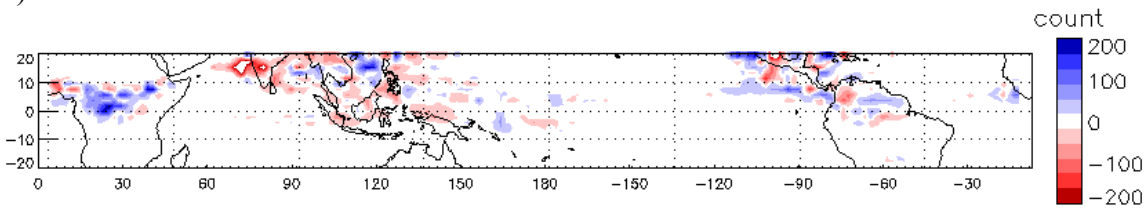

d) **SON**

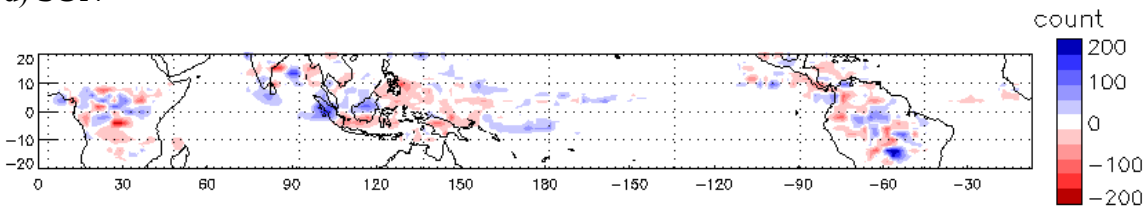

Figure 17: Monthly mean anomalous QBO west minus east 12-20 km convective echo top heights (counts) maps for a) DJF, b) MAM, c) JJA, and d) SON. Red (blue) represents an increase in convective echo top counts during the east (west) phase.

a) **DJF**

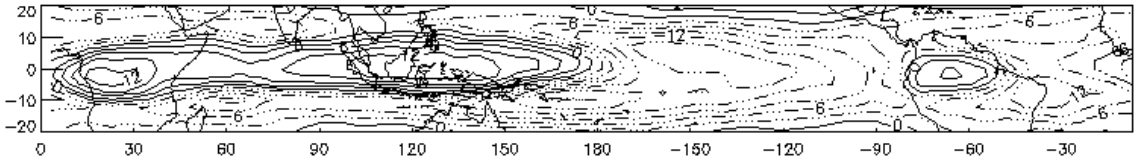

b) **MAM**

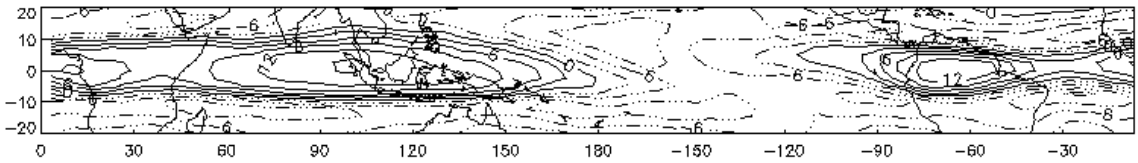

c) **JJA**

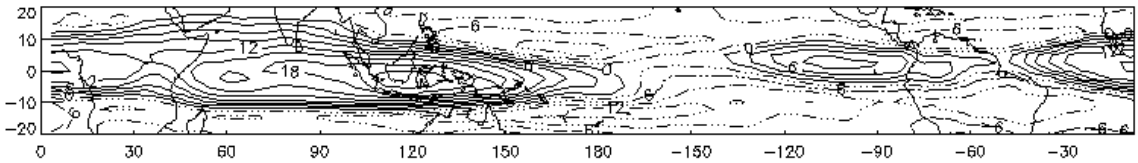

d) **SON**

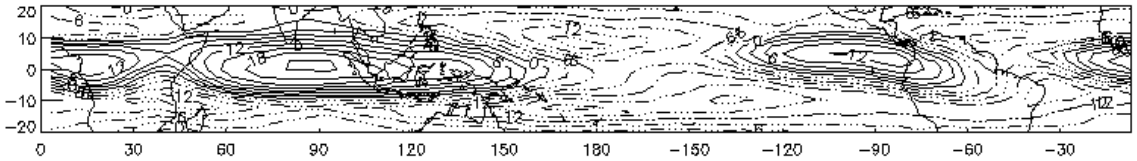

Figure 18: Monthly mean anomalous west minus east absolute 50-200 hPa shear (m s^{-1}) maps for a) DJF, b) MAM, c) JJA, and d) SON. Stronger east (west) phase shear is represented by the dashed (solid) lines.

a) **DJF**

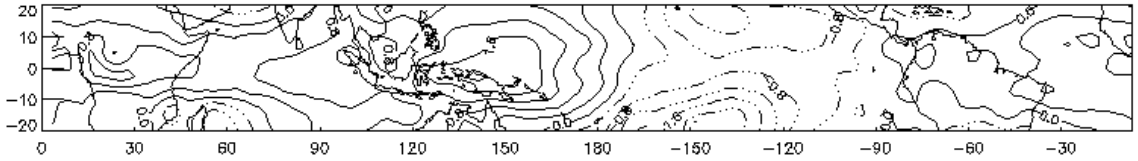

b) **MAM**

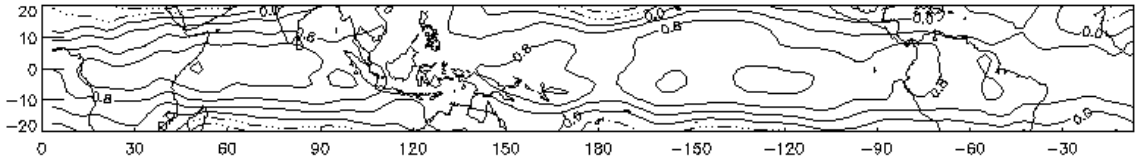

c) **JJA**

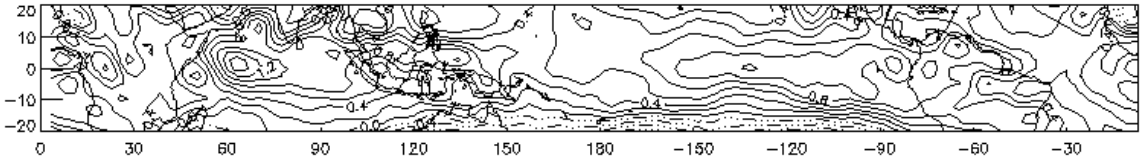

d) **SON**

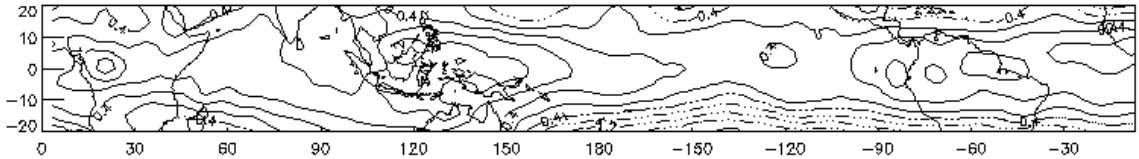

Figure 19: Monthly mean anomalous west minus east tropopause temperatures (°C) maps for a) DJF, b) MAM, c) JJA, and d) SON. Warmer east (west) phase temperatures are represented by dashed (solid) lines.

a) **DJF**

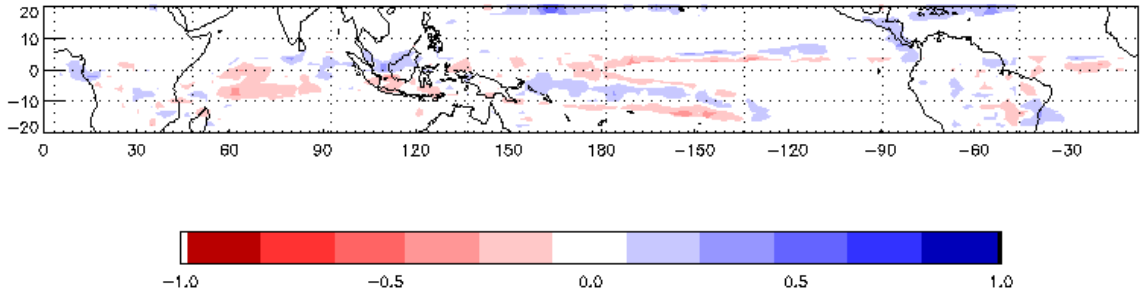

b) **MAM**

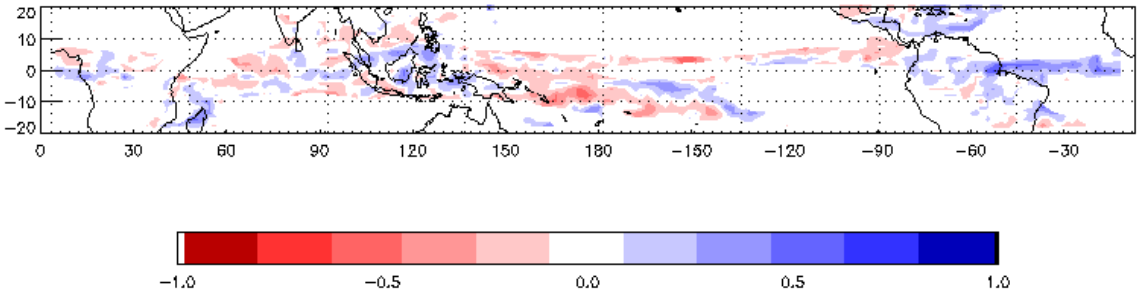

c) **JJA**

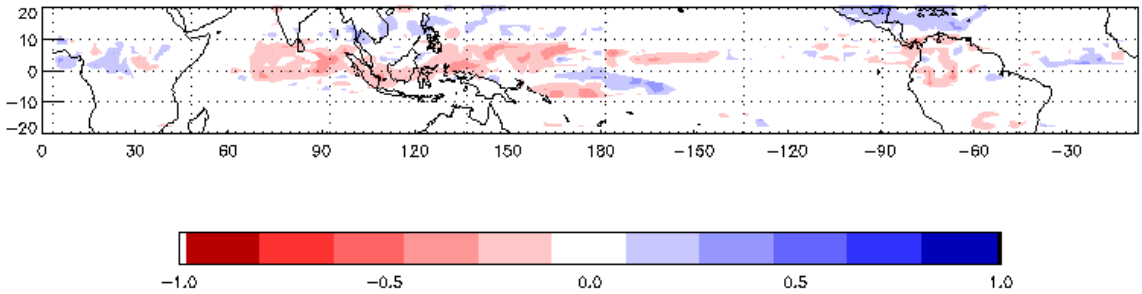

d) **SON**

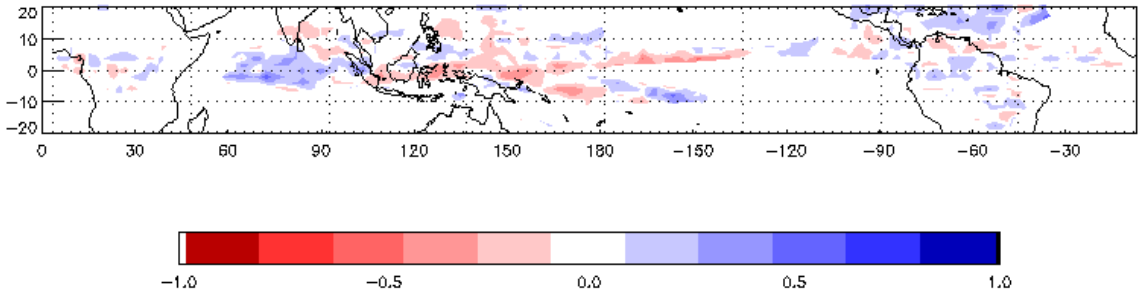

Figure 20: Correlation coefficients between anomalous absolute 50-200 hPa shear and anomalous convective rainfall for a) DJF, b) MAM, c) JJA, and d) SON. Red (blue) represents negative (positive) correlations.

a) **DJF**

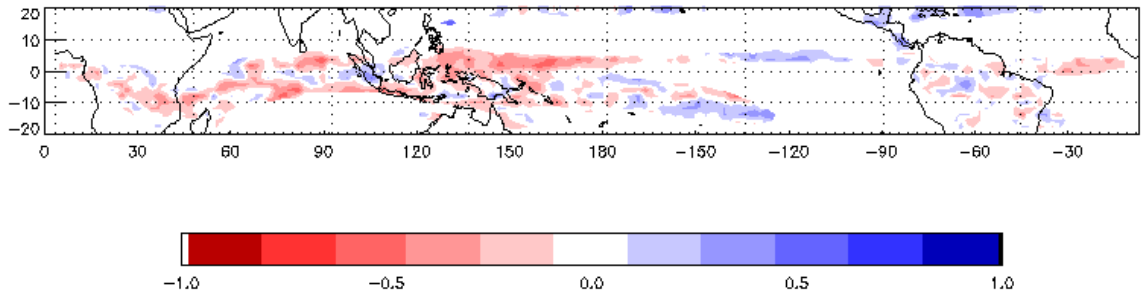

b) **MAM**

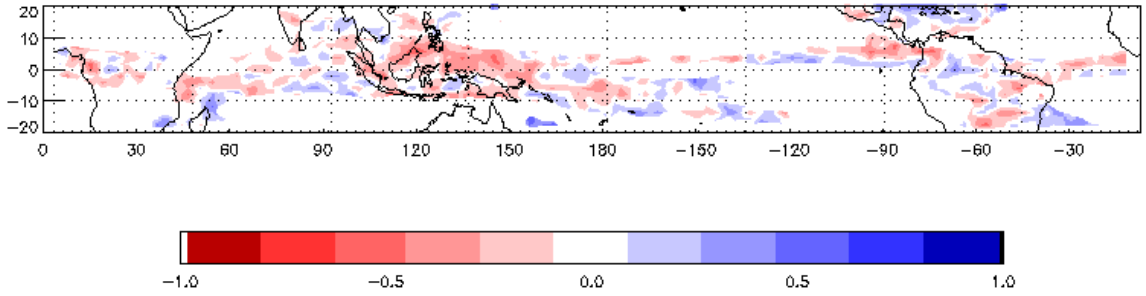

c) **JJA**

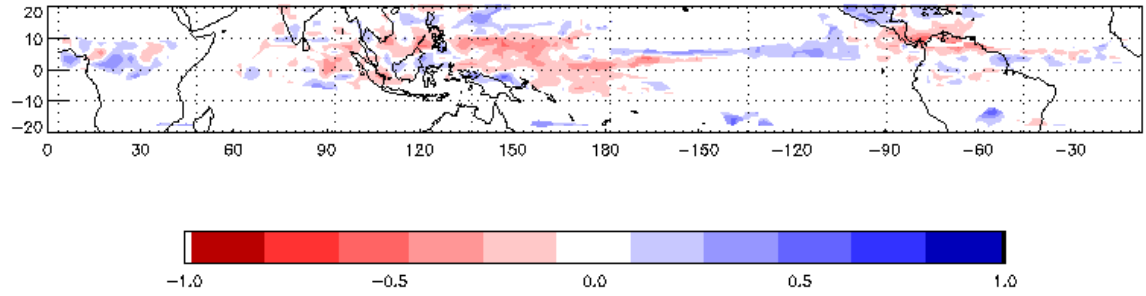

d) **SON**

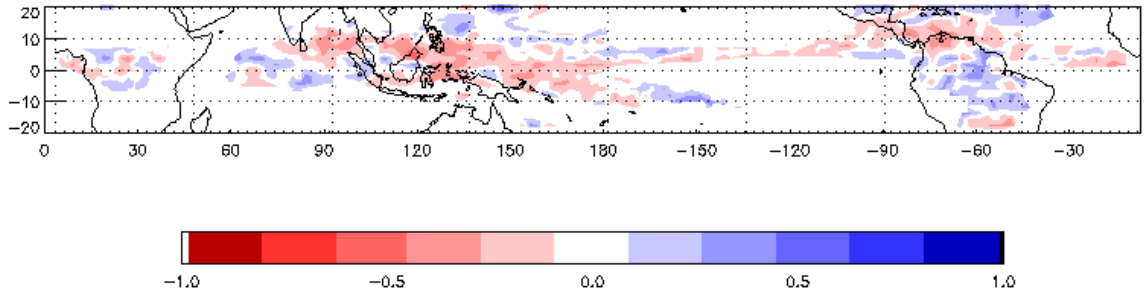

Figure 21: Correlation coefficients between anomalous tropopause temperatures and anomalous convective rainfall for a) DJF, b) MAM, c) JJA, and d) SON. Red (blue) represents negative (positive) correlations.

a) **DJF**

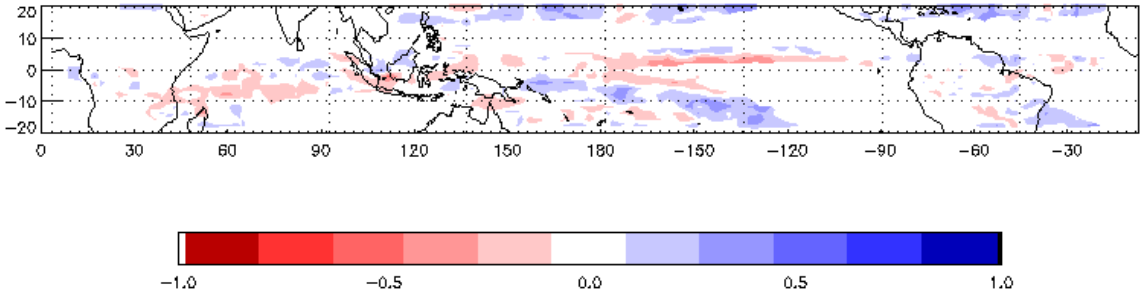

b) **MAM**

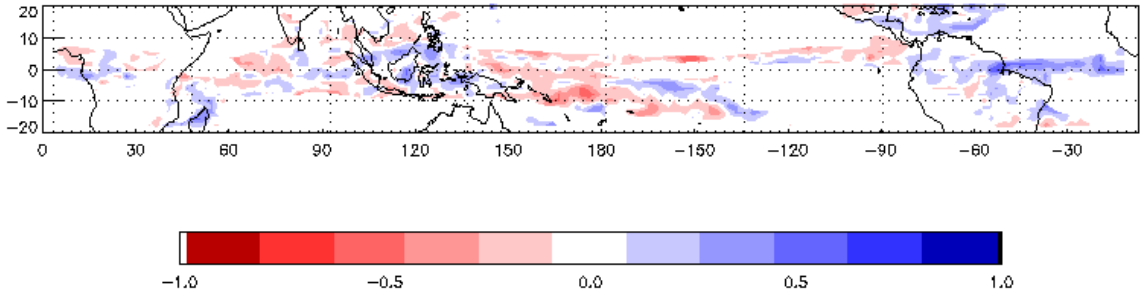

c) **JJA**

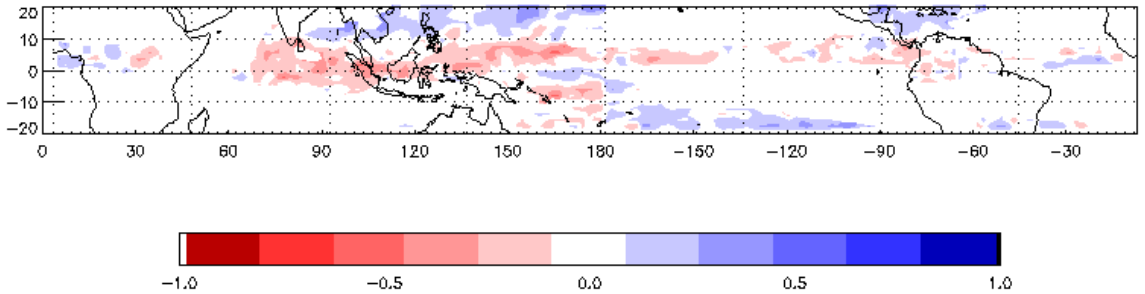

d) **SON**

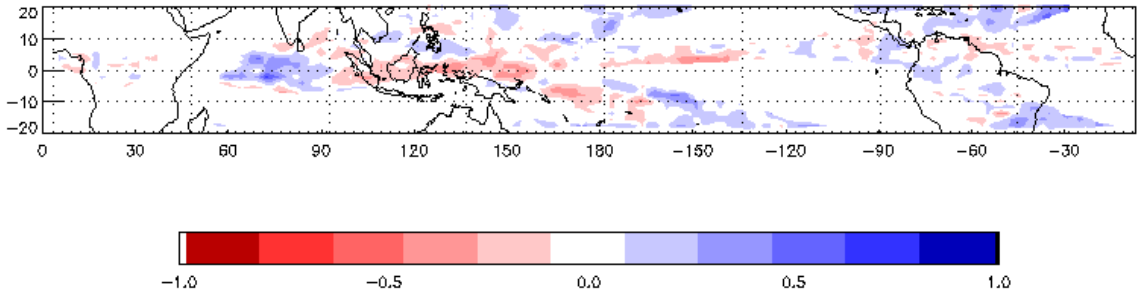

Figure 22: Correlation coefficients between anomalous absolute 50-200 hPa shear and anomalous stratiform rainfall for a) DJF, b) MAM, c) JJA, and d) SON. Red (blue) represents negative (positive) correlations.

a) **DJF**

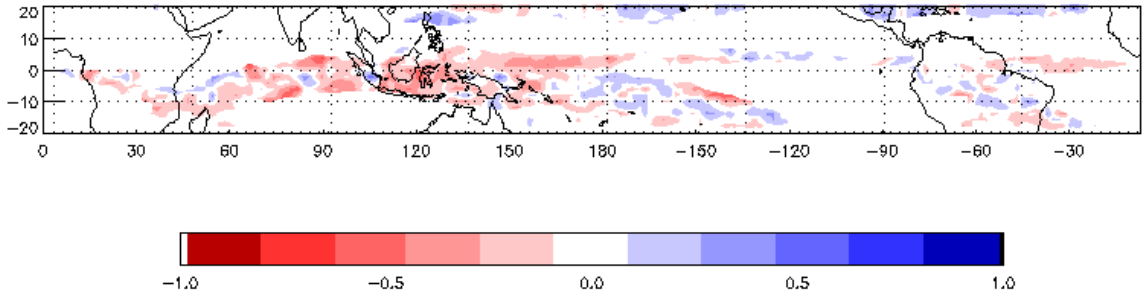

b) **MAM**

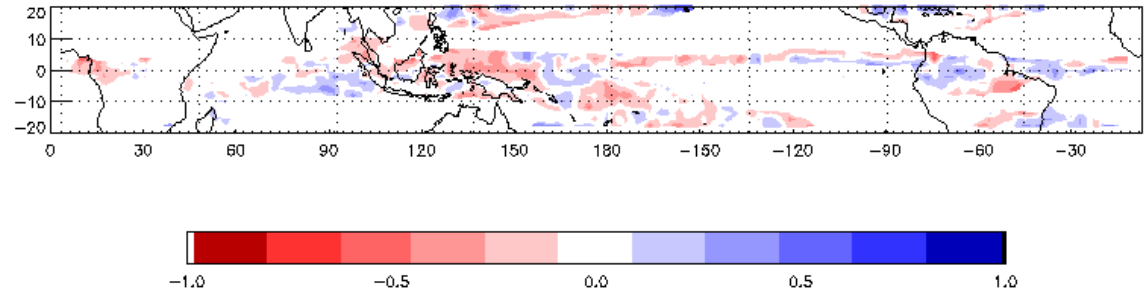

c) **JJA**

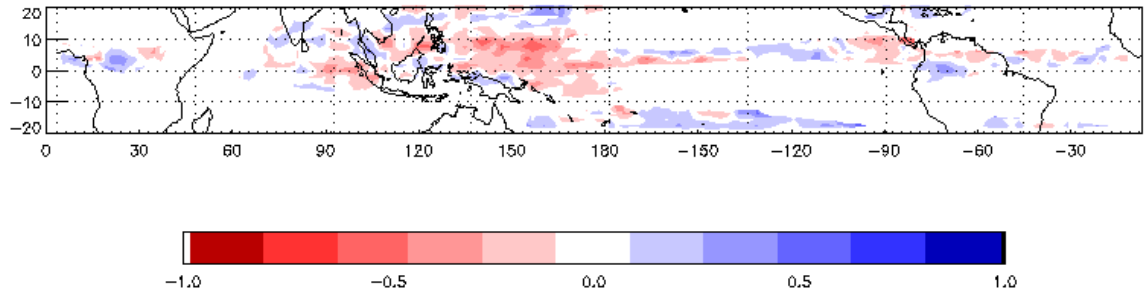

d) **SON**

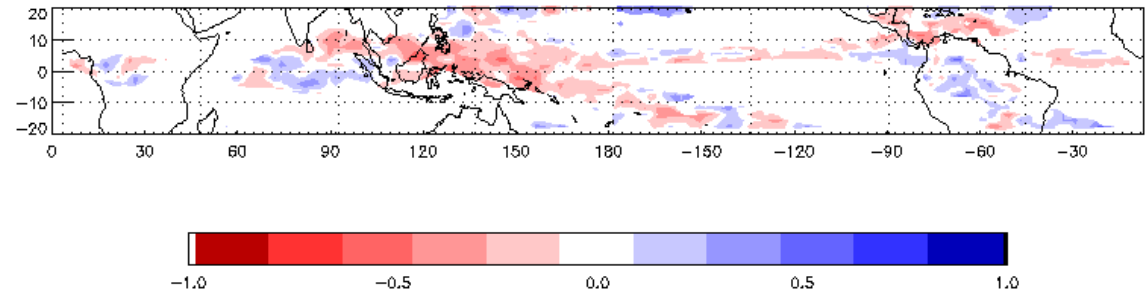

Figure 23: Correlation coefficients between anomalous tropopause temperatures and anomalous stratiform rainfall for a) DJF, b) MAM, c) JJA, and d) SON. Red (blue) represents negative (positive) correlations.

a) **DJF**

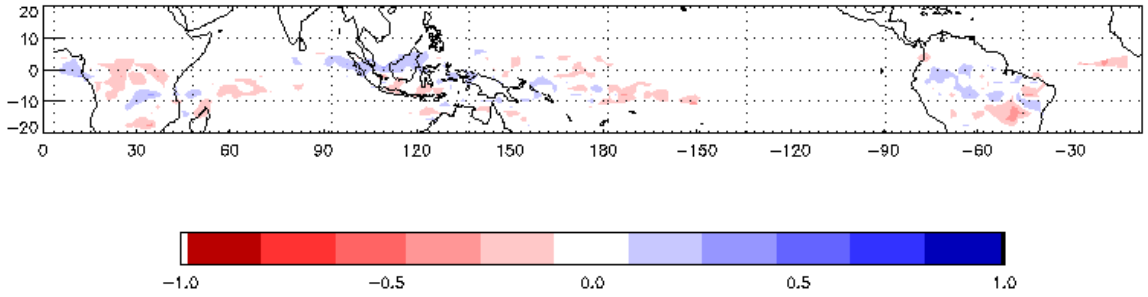

b) **MAM**

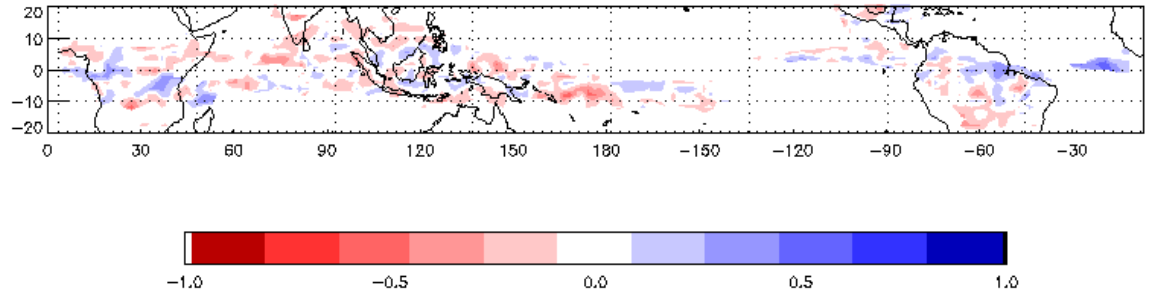

c) **JJA**

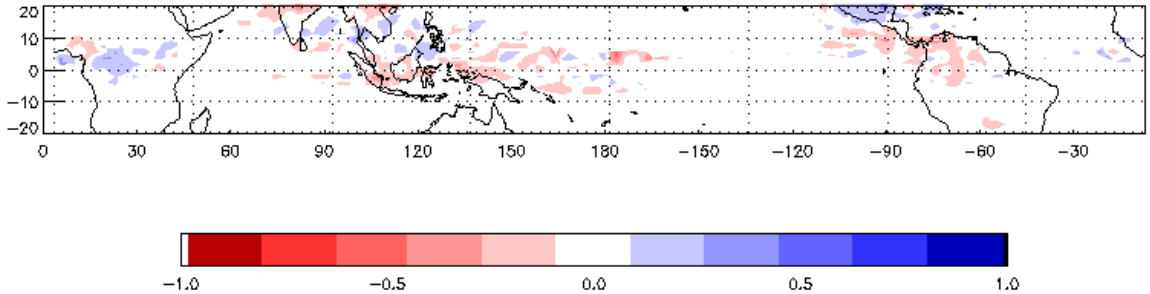

d) **SON**

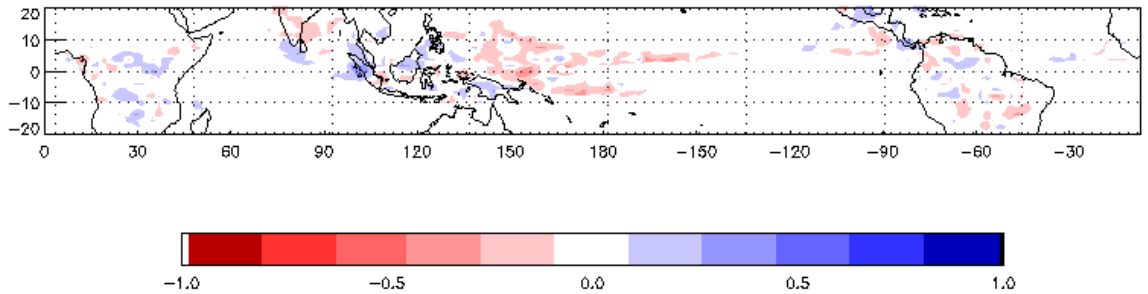

Figure 24: Correlation coefficients between anomalous absolute 50-200 hPa shear and anomalous convective echo top heights for a) DJF, b) MAM, c) JJA, and d) SON. Red (blue) represents negative (positive) correlations.

a) **DJF**

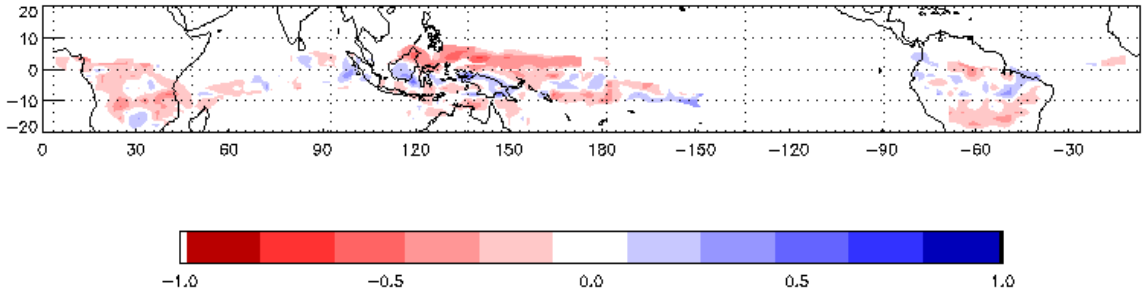

b) **MAM**

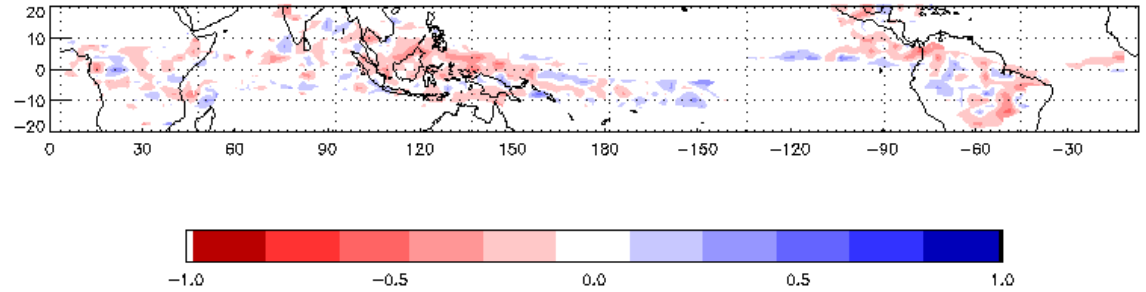

c) **JJA**

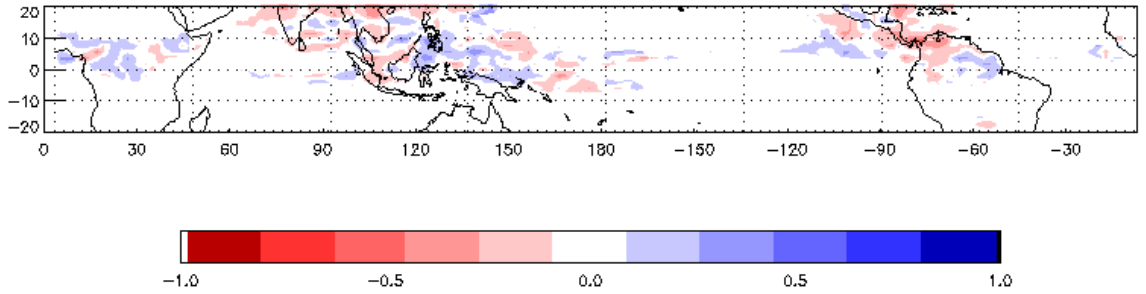

d) **SON**

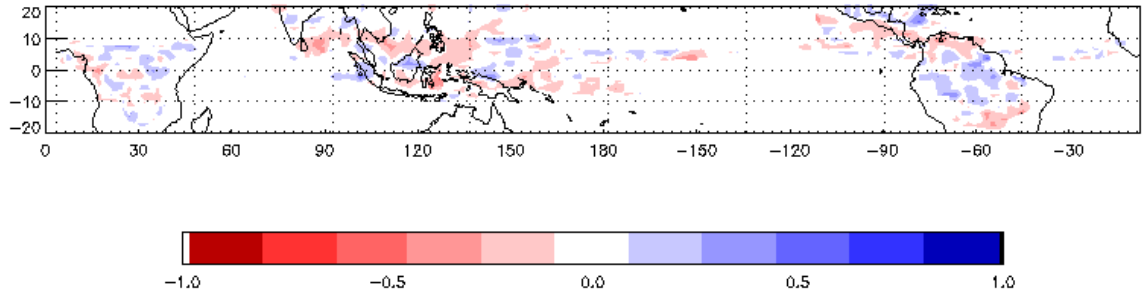

Figure 25: Correlation coefficients between anomalous tropopause temperatures and anomalous convective echo top heights for a) DJF, b) MAM, c) JJA, and d) SON. Red (blue) represents negative (positive) correlations.

Table 1: Regional and seasonal correlation coefficients between flash densities and QBO modulation of 50-200 hPa shear.

Region	DJF	MAM	JJA	SON
Africa	-0.11	0.16	0.44	0.17
India	0.19	-0.36	-0.50	-0.05
Maritime Continent/Australia	0.05	-0.18	0.32	0.48
S. America	-0.04	-0.02	-0.07	0.05

Table 2: Regional and seasonal correlation coefficients between flash densities and QBO modulation of tropopause temperatures.

Region	DJF	MAM	JJA	SON
Africa	-0.09	0.18	0.39	0.40
India	-0.12	0.28	-0.43	0.01
Maritime Continent/Australia	0.15	0.11	0.33	0.28
S. America	0.14	0.12	0.17	0.42

Table 3: Regional and seasonal correlations between convective rainfall and QBO modulation of absolute 50-200 hPa shear.

Region	DJF	MAM	JJA	SON
Africa	-0.30	0.11	0.15	-0.07
Indian Ocean	-0.02	-0.14	0.07	0.41
Maritime Continent	-0.08	-0.03	-0.25	-0.18
W. Pacific	0.24	-0.07	0.11	0.05
SPCZ	0.01	0.06	0.15	0.12
Central/S. America	0.00	0.24	0.04	0.04
E. Pacific	-0.30	-0.12	-0.23	-0.07
Atlantic	-0.25	0.43	0.09	-0.33

Table 4: Regional and seasonal correlations between convective rainfall and QBO modulation of tropopause temperatures

Region	DJF	MAM	JJA	SON
Africa	-0.06	0.03	0.07	-0.04
Indian Ocean	-0.09	-0.08	-0.01	0.17
Maritime Continent	-0.28	0.00	-0.06	-0.23
W. Pacific	-0.23	0.01	-0.03	0.21
SPCZ	0.19	0.16	-0.25	0.05
Central/S. America	-0.13	0.20	0.05	0.06
E. Pacific	0.47	-0.02	-0.08	0.10
Atlantic	0.10	0.36	-0.09	-0.22

Table 5: Regional and seasonal correlations between stratiform rainfall and QBO modulation of absolute 50-200 hPa shear.

Region	DJF	MAM	JJA	SON
Africa	-0.09	0.00	0.04	-0.04
Indian Ocean	0.02	0.01	-0.13	0.40
Maritime Continent	-0.10	0.00	-0.20	-0.52
W. Pacific	0.17	-0.17	-0.04	0.23
SPCZ	-0.07	0.08	0.14	0.15
Central/S. America	-0.03	0.30	-0.02	0.11
E. Pacific	-0.10	0.13	-0.16	0.13
Atlantic	-0.06	0.38	0.08	-0.17

Table 6: Regional and seasonal correlations between stratiform rainfall and QBO modulation of tropopause temperatures

Region	DJF	MAM	JJA	SON
Africa	-0.14	-0.02	-0.02	-0.05
Indian Ocean	-0.04	-0.04	-0.06	0.21
Maritime Continent	-0.33	0.00	0.01	-0.27
W. Pacific	-0.21	-0.04	-0.06	0.21
SPCZ	0.07	-0.13	-0.17	-0.10
Central/S. America	-0.08	0.21	0.14	0.00
E. Pacific	0.07	-0.04	-0.07	-0.13
Atlantic	0.23	0.23	-0.05	-0.14

Table 7: Regional and seasonal correlations between convective echo tops and QBO modulation of absolute 50-200 hPa shear.

Region	DJF	MAM	JJA	SON
Africa	-0.05	0.12	0.18	-0.03
Indian Ocean	-0.14	-0.16	0.24	0.09
Maritime Continent	0.01	-0.12	-0.30	-0.29
W. Pacific	0.28	-0.18	-0.11	0.09
SPCZ	0.06	-0.02	-0.07	-0.01
Central/S. America	-0.15	0.08	0.06	0.06
E. Pacific	-0.04	-0.08	-0.06	-0.01
Atlantic	-0.06	0.19	-0.05	-0.09

Table 8: Regional and seasonal correlations between convective echo tops and QBO modulation of tropopause temperatures

Region	**DJF**	**MAM**	**JJA**	**SON**
Africa	-0.09	0.11	0.11	0.01
Indian Ocean	-0.20	-0.23	0.20	0.10
Maritime Continent	-0.26	-0.09	-0.21	-0.30
W. Pacific	-0.19	-0.16	0.03	-0.03
SPCZ	0.05	-0.08	-0.07	0.01
Central/S. America	-0.12	0.02	0.04	0.06
E. Pacific	0.27	-0.17	-0.03	0.06
Atlantic	0.07	0.20	-0.06	-0.09

VITA

Name: Celina Anne Hernandez

Address: 5335 Calistoga San Antonio, TX 78228

Email Address: celah02@tamu.edu

Education: B.S., Meteorology, Texas A&M University, 2006
M.S., Atmospheric Sciences, Texas A&M University, 2008